Journal of Earthquake Engineering, 20:699–737, 2016

ISSN: 1363-2469 print / 1559-808X online
DOI: 10.1080/13632469.2015.1104747

Taylor & Francis
Taylor & Francis Group

Selection of Ground Motion Prediction Equations for Seismic Hazard Analysis of Peninsular India

P. ANBAZHAGAN[1,2], M. SREENIVAS[1], B. KETAN[1], S. S. R. MOUSTAFA[2,3], and N. S. N. AL-ARIFI[2]

[1]Department of Civil Engineering, Indian Institute of Science, Bangalore, India
[2]Geology and Geophysics Department, King Saud University, Riyadh, Saudi Arabia
[3]Seismology Department, National Research Institute of Astronomy and Geophysics (NRIAG), Cairo, Egypt

Seismic hazard analysis provides an estimation of seismic hazard parameters like peak ground acceleration (PGA) or spectral acceleration (SA) for different periods. The extent of ground shaking and the hazard values at a particular region are estimated using ground-motion prediction equations (GMPEs)/attenuation equations. There are several GMPEs applicable for the region to estimate the PGA and SA values. These equations may result in higher or lower PGA and SA values than the region specific reported values, which are based on the parameters involved in the development of GMPEs. In this study, an attempt has been made to identify the best GMPEs for various parts of Peninsular India (PI) by performing an "efficacy test," which make use of the average log likelihood value (LLH). Various intraplate earthquakes such as Coimbatore earthquake, Satpura earthquake, Anjar earthquake, Koyna earthquake, Bhadrachalam earthquake, Broach earthquake, Shimoga earthquake, Killari earthquake, Jabalpur earthquake, Pala earthquake, Kottayam earthquake, and Bhuj earthquake have been considered for the same. Macroseismic intensity maps of these earthquakes have been digitalized and European Macroseismic Scale (EMS) values at the surface have been synthesized. PGA value determined from each GMPE for known magnitude and hypocentral distances are then converted to EMS values. These calculated EMS values have been used to estimate LLH values which are further used to compute Data Support Index (DSI), rank and weights corresponding to a particular GMPE. Conventionally, LLH values are estimated for the entire distance range and GMPEs are ranked accordingly, but in this study, the LLH is calculated for the distance segments of 0-200 km and 200 km to maximum damaged distance in the region based on Isoseismal maps. If the maximum damaged distance is less than 200 km, a distance segment up to 200 km is adopted. Comparison between the rankings of the GMPEs in segments 0–200 km and 200–maximum damage distance is presented here. Segment-based GMPEs ranking shows different ranks, DSI and weights for each GMPE as compared to ranking considering entire distance. Finally, this study provides a list of GMPEs that perform best for the estimation of ground motion parameters in different parts of PI. This study shows that the GMPEs of HAHO-97, ATK-08, CAM-06, TOR-02, NDMA-10, and PEZA-11 perform better for the estimation of ground motion in most part of PI in the distance segment 0–200 km. The GMPEs of TOR-02, RAIY-07, and RAIY-07 (PI) perform best in the 200-maximum damage distance segment.

Keywords Ground-Motion Prediction Equation; LLH; EMS; PGA; PI

1. Introduction

India has experienced several devastating earthquakes in the past and has witnessed severe damage to property and loss of lives. The effects of earthquakes can be minimized by

Received 19 July 2014; accepted 21 August 2015.
Address correspondence to P. Anbazhagan, Department of Civil Engineering, Indian Institute of Science, Bangalore, India. E-mail: anbazhagan2005@gmail.com
Color versions of one or more of the figures in the article can be found online at www.tandfonline.com/ueqe.

determining the seismic hazard and the strong motion that has been produced by earthquake events in various parts of the country and designing the structures accordingly. Ground-motion or vibration produced by earthquakes cause immense structural damages and to reduce these damages, engineers demand the design ground-motion for designing of structures. Hence, the knowledge of appropriate strong ground-motion is essential to assure the safety of structures like power plants, dams, bridges, etc. and to decide the design ground-motion at a particular region. Distribution of strong ground-motion parameters at a particular region can be determined by using the appropriate Ground Motion Prediction Equation (GMPE) which is valid for that seismic study area (SSA).

An important step in any seismic hazard analysis study is the selection of suitable Ground-Motion Prediction Equations (GMPEs) based on the region specific parameters. These are widely used for predicting the level of ground shaking in seismic hazard analysis. GMPEs are the mathematical equations which relate the ground-motion parameters like Peak Ground Acceleration (PGA), Spectral Acceleration (SA), etc., with region-specific seismological parameters like magnitude (moment magnitude, in most of the cases), distance (epicentral or hypocentral), site condition, and type of faulting. These equations are widely used to estimate the seismic hazard values at bedrock and surface for a particular regions for a range of time periods. GMPEs play an important role in evaluating the liquefaction hazard, earthquake-resistant design of structures and determining the earthquake-induced forces that can lead to instability of earth structures, etc. The basic component of Probabilistic Seismic Hazard Analysis (PSHA) is an integration of a suitable attenuation model for the estimation of ground-motion parameters of a given site for each earthquake scenario. Appropriate GMPE to calculate the ground-motion in terms of PGA or SA is a pre-requisite for any type of seismic hazard analysis for a particular SSA. Availability of large number of GMPEs demands selection of suitable GMPEs for a region. However, the selection and ranking of appropriate models for a particular target area often pose serious practical problems [Scherbaum *et al.*, 2004]. Qualitative and quantitative methods are available to select suitable GMPEs for any region. Cotton *et al.* [2006] gave a list of guidelines on rejecting ground motion equations. Scherbaum *et al.* [2004] used exceedance probabilities for selection and ranking of the GMPEs. Scherbaum *et al.* [2009] improved previous work and proposed an information-theoretic approach for ranking of GMPEs considering Log Likelihood (LLH) estimates. The aim of this study is to identify suitable GMPEs for different parts of Peninsular India and determining the ranking and weight for seismic hazard analysis by considering the available data of region specific earthquake Isoseimal maps and GMPEs.

Eleven applicable GMPEs for PI have been considered for this study. Of these, three were developed in the region and eight were developed elsewhere for a similar seismotectonic region. Past earthquake damage distribution, i.e., intensity maps have been collected for different parts of PI and are used in this study. The intensity values obtained from isoseismal maps are converted to PGA values as less number of recorded data (PGA) is available of corresponding earthquakes. Some of the GMPEs can better estimate PGA/SA values for a particular distance segment and is not applicable for higher distance segments because of its limitation on magnitude and distance. Hence, maximum damaged distance for the past earthquake is divided into segments of 0–200 km and 200 km-maximum damage distance. PGA values are estimated for each distance bin by considering 11 GMPEs for each of the earthquake and then converted to European Macroseismic Scale (EMS) values. These EMS values are further used to estimate LLH values and Data Support Index (DSI), which are further used to compute the rank and weights for GMPEs considering each region/past earthquake location. Segmented-based ranking of GMPEs is attempted in order to avoid over/under estimation of the PGA at shorter and longer distances. Comparison

between rankings for different segments viz. 0–200 km and 200-maximum damage distance show that the ranking of a particular GMPE differ with the segment considered. Therefore, GMPEs suitable for segment 0–200 km need not be suitable for segment 200-maximum damage distance.

2. Geological Background of PI

The geological formation of Peninsular India (PI) is considered as one of the oldest landmasses of the earth's crust. Most of the PI is classified as Gneissic complex/Gneissic granulite with major inoculation of greenstone and allied supracrustal belt. The geological deposits close to the eastern and western side of the study area is coastline having the alluvial fill in the pericratonic rift. The major tectonic constituents in the Southern India include the massive Deccan Volcanic Province (DVP), South Indian Granulite Terrain (SIGT), Dharwar craton (DC), Cuddapah basin (CB), Godavari Graben (GG), Mahanadi Graben (MG), and the Eastern and the Western Ghats on the east and west coast of India, respectively [Anbazhagan, 2007]. Figure 1 shows geological setting of PI along with earthquakes considered in this study. The South Indian Granulite Terrain consists of three high-grade metamorphic blocks joined by series of shear zones namely Moyar Bhavani shear zone, Palghat Cauvery shear zone, and Achankovil shear Zone. These zones divide the SIGT terrain into Northern Block, Nilgiri Block, Madras Block, Madurai Block, and Trivandrum Block [Meert *et al.*, 2010]. The Northern block is also called as the Salem block and is situated below Dharwar Craton, and consists of Charnockites, Granite Gneisses, and Migmatites. The Nilgiri Block consists of Garnetiferous rocks, Kyanite Gneisses, and quartzite are also distributed throughout the block [Raith *et al.*, 1999]. The Madras block is located in the east of Nilgiri-block and it consists of medium to high-pressure charnockites and gneisses that were pressed into long and thin bands. This block also includes Madukkarai super crustals, which display complex broad doming [Chetty and Rao, 2006]. The Madurai Block is the largest in the whole South Indian Granulites blocks. The western region mostly consists of charnockite massifs whereas the eastern region mainly consists of basement gneisses and related meta sedimentary complexes [Braun *et al.*, 2007].

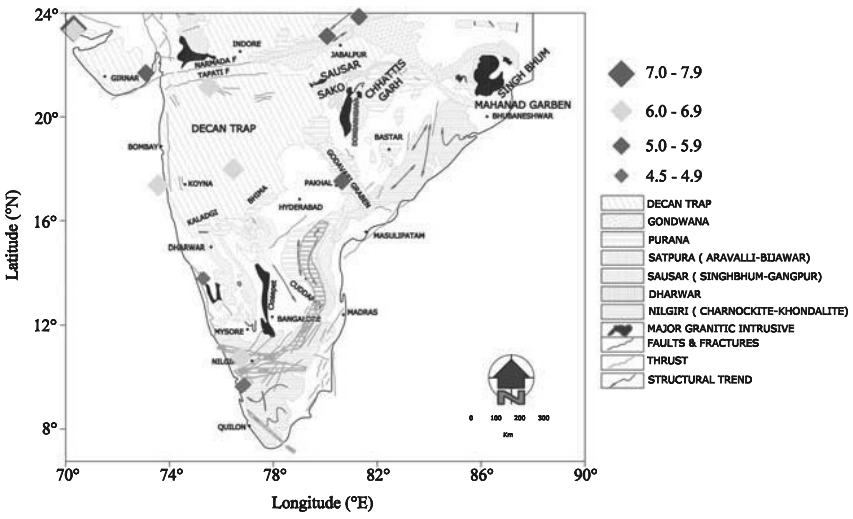

FIGURE 1 Geology map of south India with past earthquakes considered in this study.

The Trivandrum Block is comprised of sillimanite granulites, garnet-biotite gneisses, and calc-silicates. It also contains a large charnockite massif which is named as Nagarcoil block [Santosh *et al.*, 2006]. The Eastern Ghats region consists of two rift valleys mainly Mahanadi rift in the north and Godavari rift in the south [Biswal *et al.*, 2007]. It comprises of metapelite and enderbetic gneisses and enderbitic and charnokitic intrusions [Stein *et al.*, 2004]. This region is generally a stable zone characterized by low magnitude shallow focus earthquakes and occasional 5–6 magnitude earthquakes.

The Dharwar Cratons is divided into Eastern and Western Dharwar Cratons because of the differences in the abundance of greenstones and the degree of regional metamorphism [Rollinson *et al.*, 1981]. The Eastern Dharwar Craton is composed of Dharwar batholith, greenstone belts, intrusions, and sedimentary basins. The Dharwar batholith comprises of series of plutontic belts. These belts are 15–25 km wide and hundreds of km long, predominantly trending from North west to Southeast. They are mainly mixtures of juvenile multiple granites and diorites. These mixtures form a wedged shape with granitic dyke intrusions. The Greenstone and schists belt are concentrated at the West and are covered by the Cuddapah Basin in the East. The metamorphism of the belt ranges from greenschist to amphibolite facies. Mafic dykes, kimberlites, and lamprotites represent most of the intrusions in the Eastern Dharwar craton. The intrusions around the Cuddapah basin have NW-SE, E-W, and NE-SW trends. These Dyke intrusions disappear beneath the Cuddapah basin. The Western Dharwar is located in the South West India. The northern region was buried under the Deccan traps. The western Dharwar Craton mainly consists of Archaen Tonalitic Trondhjemitic Granoditic Gneisses.

The Cuddapah basin is located in the eastern portion of the eastern Dharwar Craton, the eastern border of this basin is represented as a thrust boundary and Epi-Archaen unconformity [Meert *et al.*, 2010] represents the other boundaries. The sediments are approximately 12 km thick and is made up of two stratigraphic groups namely the Cuddapah super group and Kurnool group. The Kurnool group has unconformably deposited over the Cuddapah super group. The basin is surrounded by granitic gneisses, dykes, and sills, which terminate at the boundary [Meert *et al.*, 2010]. The Pranhita-Godavari basin is one of the ancient basins and is situated between Dharwar and Bastor Cratons. The sedimentary sequence within the basin consists of a series of unconformity bound packages. Based on the classifications given, the sediments are collectively known as the Godavari super group [Chaudhuri, 2003], which consists of three unconformity-bounded groups namely Pakhal group, Albaka group, and Sullavai group. The Pakhal group represents the southwest region of the basin and consists of two subgroups called Mallampalli and Mulug. Mallampalli subgroup mainly consists of limestone and quartz arenite. The Mulug subgroup consists of basal conglomerate followed by carbonate-rich shelfal sequence. Albaka subgroup consists of sandstones and shales which unconformably overly the Pakhal group. Sullavai group consist of sandstone and conglomerate which forms the uppermost subgroup [Chaudhuri, 2003]. Available geological setting of PI is a broader picture and not much importance is given to micro level geological mapping. Changes in seismic wave propagation, however, can be noticed because of the change in geological formation.

3. Seismic Hazard Assessment Studies in PI

PI was once believed to be a stable region but is not stable anymore. Deadliest stable continent earthquake, i.e., Latur Earthquake 1993 was reported in Indian Peninsular [Gupta, 2006]. Sequences of many damaging earthquakes (see Table 1) in the last century have occurred in the Indian Peninsula. The conference on SCR earthquakes on 1998 discussed several issues and highlighted the seismic events at stable continent area throughout the world. Further, it was suggested that the SCR is much more vulnerable to earthquakes

TABLE 1 Data of the earthquakes considered in the study

Sl. No.	Earthquakes	Year	Moment Magnitude (M_w)	Focal Depth (km)	Maximum Damaged Distance [km]
a	Coimbatore earthquake	1900	6.0	70	500
b	Satpura earthquake	1938	6.3	40	600
c	Anjar earthquake	1956	6.0	15	300
d	Koyna earthquake	1967	6.3	8	300
e	Bhadrachalam earthquake	1969	5.7	17	400
f	Broach earthquake	1970	5.4	8	300
g	Shimoga earthquake	1975	4.7	35	300
h	Killari earthquake	1993	6.1	5	300
i	Jabalpur earthquake	1997	5.8	36	300
j	Pala earthquake	2000	4.7	7	300
l	Bhuj earthquake	2001	7.6	25	400

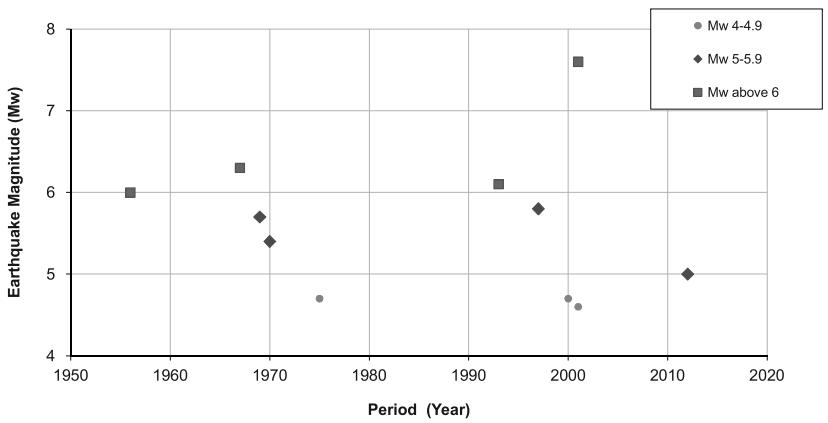

FIGURE 2 Earthquake with Isoseismal map considered in this study.

than it was once thought [Gupta, 2006]. In India, the SCR is experiencing damaging earthquakes more frequently as compared to active seismic regions of India. Figure 2 shows the plot of earthquake events that caused building damages (intensity of above 4). It can be noted from Fig. 2 that minimum of one earthquake has occurred in each decade except 1980–1990 for the past seven decades. Similarly, in the last six decades analysis showed that occurrence of minimum of two earthquakes in every decade except 1980–1990 where no earthquake was reported. It can also be noted that several tremors are being reported in many parts of PI after the big Sumatra earthquake of 2004. However, seismic hazard analysis of Peninsular India at surface level is neither attempted systematically nor understood at a microscale level. Primary step towards developing seismic zonation standards for seismic design or retrofitting of structures and seismic disaster management is estimating the seismic hazard precisely. Seismic hazard are estimated deterministically, in which a particular earthquake scenario is assumed, or probabilistically, in which uncertainties in

earthquake size, location, and time of occurrence are explicitly considered [Kramer, 2003; Anbazhagan *et al.*, 2012]. Seismicity of PI was presented by many researchers and predominantly by Chandra [1977], Rao and Rao [1984], Srivastava and Ramachandran [1985], Guha and Basu [1993], Jaiswal and Sinha [2007a,b, 2008], Anbazhagan [2007], Menon *et al.* [2010], NDMA [2010], Martin and Szeliga [2010], Szeliga *et al.* [2010], Kolathayar and Sitharam [2012], and Nath and Thingbaijam [2012]. Different seismic hazard studies has considering different GMPEs in analysis are also studied and presented.

Seismic zonation of PI started in 1960s as a part of Indian seismic zonation map for Indian Standard IS1893-2002. These zonations are based on earthquake epicenters, isoseismal map and is being revised soon after every major earthquake in the country. Seismic zonation should be based on region specific seismic hazard analysis being a prime input for national standards; however, very limited attempt has been made to develop such maps for entire India. Basu and Nigam [1977], Khattri *et al.* [1984], Bhatia *et al.* [1999], NDMA [2010], and Nath and Thingbaijam [2012] preformed a probabilistic seismic hazard analysis of India on a macroscale level and presented seismic zonation map. PI is experiencing earthquake since historic times but systemic seismic hazard estimation of PI was carried out only after 1980s and region specific seismic hazard analysis studies were started after 2007. GMPEs should be considered to arrive hazard values in the each seismic hazard analysis are listed in Table 2. Additionally, weight factor and ranks corresponding to different GMPEs adopted in each study is also given in Table 2. It had been observed that, in most of the studies the region-specific GMPE developed by Raghukanth and Iyengar [2007], is considered as superior and given more weights in logic tree construction for seismic hazard analysis. Moreover, few studies have used GMPEs developed for region other than SCR-like active seismic region and more details about these can be found in Nath and Thingbaijam [2011]. From Table 2, it is clear that handling of GMPEs are not consistent with respect to its ranking and weights in most of the seismic hazard studies, as these are important in predicting reasonably accurate hazard values at site.

4. Past Earthquakes in PI

PI had experienced several earthquakes having magnitude moment (M_w) more than 5 and 12 earthquakes with M_w greater than 6. Isoseimal maps are available for selected earthquakes, which are very much useful in seismic hazard analysis studies in PI. In this study, Coimbatore Earthquake (1900), Satpura Earthquake (1938), Anjar Earthquake (1956), Koyna Earthquake (1967), Bhadrachalam Earthquake (1969), Broach Earthquake (1970), Shimoga Earthquake (1975), Killari Earthquake (1993), Jabalpur Earthquake (1997), Pala Earthquake (2000), Kottayam Earthquake (2001), and Bhuj Earthquake (2001) has been considered to identify the best suitable GMPEs. The magnitudes, focal depths, and macroseismic intensity maps of all the earthquakes were obtained from http://www.seismosoc.org. Table 1 shows moment magnitude, focal depth and maximum distance where intensity value of 4 and above were reported for these earthquakes. Figure 1 shows the location of these earthquakes along with geological background. A brief summary of each earthquake event is presented below.

4.1. Coimbatore Earthquake

The most damaging event of Coimbatore occurred on February 8, 1900 with a moment magnitude of 6.3 and focal depth of 70 km. A maximum intensity value of VII was reported

TABLE 2 Seismic hazard analysis carried out for Peninsular India with GMPEs used

Study Area	Reference	GMPE/s used for Peninsular India	Weights used GMPE/s
Entire India	Khattri *et al.* [1984]	Algermissen and Perkins [1976]	1.00
Entire India	Bhatia *et al.* [1999]	Joyner and Boore [1981]	1.00
Entire India	NDMA [2010]	Indigenously developed	1.00
		Toro [2002]	0.25
		Campbell [2003]	0.25
Entire India	Nath and Thingbaijam [2012]	Atkinson and Boore [2006]	0.25
		Raghukanth and Iyengar [2007]	0.25
Entire India	Kolathayar and Sitharam [2013]	Atkinson and Boore [2006]	0.33
		Raghukanth and Iyengar [2007]	0.33
		Campbell and Bozorgnia [2008]	0.33
Entire India	Sitharam and Kolathayar [2012]	Raghukanth and Iyengar [2007]	1.0
Entire India	Ghosh *et al.* [2012]	NDMA [2010]	0.50
		Atkinson and Boore [2006]	0.50
Gujarat	Petersen *et al*. [2004]	Frankel *et al.* [1996]	0.50
		Toro *et al.* [1997]	0.50
Peninsular India	Jaiswaland Sinha [2007a]	Iyengar and Raghukanth [2004]	0.50
		Atkinson and Boore [1995]	0.25
		Toro *et al.* [1997]	0.25
Eastern coast of India	Kanagarathinam *et al.* [2008]	Iyengar and Raghukanth [2004]	1.00
Bangalore	Anbazhagan *et al.* [2009]	Iyengar and Raghukanth [2004]	1.00
South India	Vipin *et al.* [2009]	Raghukanth and Iyengar [2007]	1.00
		Atkinson and Boore [1997]	0.10
NPP site in peninsular India	Roshan and Basu [2010]	Abrahamson and Silva [1997]	0.25
		Boore *et al.* [1997]	0.25
		Campbell [1997]	0.15

(*Continued*)

TABLE 2 (Continued)

Study Area	Reference	GMPE/s used for Peninsular India	Weights used GMPE/s
		Sadigh *et al.* [1997]	0.25
		Abrahamson and Silva [1997]	0.33
Tamil Nadu	Menon*et al.* [2010]	Campbell and Bozorgnia [2008]	0.33
		Raghukanth and Iyengar [2007]	0.33
Chennai	Ramanna and Dodagoudar [2012]	Raghukanth and Iyengar [2007]	1.00
Surat City, Gujarat	Thaker *et al.* [2010]	Iyengar and Raghukanth [2004]	1.00
Coimbatore	Anbazhagan *et al.* [2012]	Raghukanth and Iyengar [2007]	1.00
Visakhapatnam	Lalith Kumar *et al.* [2012]	Joyner and Boore [1981]	1.00
		Raghukanth and Iyengar [2007]	0.40
Karnataka State	Sitharam *et al.* [2012]	Atkinson and Boore[2006]	0.30
		Toro [2002][TOR02],	0.30
		Raghukanth and Iyengar [2007]	0.20
		Abrahamson and Silva [1997]	0.133
Ports of Gujarat	Shukla and Choudhury [2012]	Frankel *et al.* [1996]	0.133
		Toro *et al.* [1997]	0.133
		Boore-Joyner-Fumal [1997]	0.133
		Campbell [1997]	0.133
		Sadigh *et al.* [1997]	0.133
		Abrahamson and Silva [1997]	0.30
Kancheepuram	Corigliano *et al.*[2012]	Campbell and Bozorgnia [2008]	0.30
		Raghukanth and Iyengar [2007]	0.40

near to the epicenter region. The earthquake was felt throughout southern India, south of 14°N, over an area of 25,000 km^2. The epicentre was located at 10.75° North Latitude and at 76.75° East Longitude. This region consists of south western part of Mysore region in Karnataka, northwestern parts of Tamil Nadu, and parts of Kerala between Alleppy and Cannanore, districts with the major centres being Bangalore, Mysore, Mangalore, Erode, Coimbatore, Rajyapalayam, Calicut, Palaghat, Trichur, and Ernakulam. Kaveri and Periyar along with the west flowing rivers of Western Ghats form the major river basins. Isoseismal map of Coimbatore earthquake is given in Fig. 4. From Fig. 4, it can inferred that maximum distance of damage is about 500 km.

4.2. Satpura Earthquake

Satpura earthquake of March 14, 1938 struck with a moment magnitude of 6.3 and a focal depth of 40 km, near the Khandwa region within the Son-Narmada-Tapti (SONATA) zone. The epicentre was located at 21.16° N and 75.52° E. This earthquake was located at the hills in central India and felt up to eastern Gujarat and also runs through Maharashtra, Madhya Pradesh, and Chattisgarh. The earthquake Isoseismal map covers a major part of Madhya Pradesh and parts of Maharashtra which includes Ujjain, Rajgarh, Betul, Guna, and Khandwa of Madhya Pradesh and Bhushwal of Maharashtra with Narmada, Tapti, and Chambal being the major rivers. The seismogenic area can be broadly divided into two tectonic blocks viz. the northern Bundelkhand block and the Son-Narmada-Tapti (SONATA) lineament zone separated by the ENE-WSW trending Son Narmada South Fault, which has been active since the late Archaean period [Tewari *et al.*, 2001].

4.3. Anjar Earthquake

Anjar earthquake occurred on July 21, 1956 and had a magnitude (Mw) of 6.0. The maximum intensity was recorded to be IX (MM scale). The epicentre was located at 23.33° N and 70.32° E. The radius of perceptibility was about 300 km and the focal depth was 15 km. It caused considerable damage to a number of villages in the Anjar region near the central mainland of Kutch. About 115 people were killed, hundreds were injured, and 1,350 houses were destroyed in Anjar town alone. The area suffered maximum damage of about 2,000 km^2.

4.4. Koyna Earthquake

Koyna Earthquake occurred on December 10, 1967 with the moment magnitude of 6.3 and focal depth of 8 km. The epicentre was located at 17.36° N and 73.57° E. The earthquake damaged area covered western Maharashtra, southern Gujarat, and Union Territory of Daman. This includes certain cities like Mumbai, Pune, Nasik, Ahmadnagar, and Daman and the Western Ghat Hill Range forms the main water division of this area from major west-flowing rivers such as Vaitarna and Vashist and east flowing Godavari, Ghod, Koyna, Mula, and Krishna.

4.5. Bhadrachalam Earthquake

The major earthquake of Bhadrachalam occurred on April 13, 1969 with the main shock having a moment magnitude of 5.7 and focal depth of 17 km. The epicenter was located at 17.52° N 80.64° E. The damage area encompasses a major portion of the Telangana region of Andhra Pradesh and a small south eastern part of Maharashtra with the major cities

being Hyderabad, Warangal, Karimnagar, Khammam, and Adilabad of Andhra Pradesh and Chandrapur of Maharashtra. Godavari River Basin with major tributaries such as Pranhita and Indravathi were completely affected by this earthquake.

4.6. Broach Earthquake

An earthquake shock of moment magnitude 5.4 and focal depth of 8 km severely rocked the old town of Broach on the morning of March 23, 1970. The epicenter was located at 21.69°N and 73.09°E. From the survey of damages, an intensity of 8 in MMI scale was observed at the epicentre area. Macroseismic survey of the affected area revealed that the extensive damages were mainly confined to the northern bank of river Narmada. The quake caused injures of about 100 persons and destroyed 26 structures.

4.7. Shimoga Earthquake

Shimoga Earthquake of May 12, 1975 was an interesting earthquake that occurred with a moment magnitude of 4.7 and the maximum intensity was reported to be V. The focal depth and felt radius were 35 km and 140 km, respectively. The epicenter was located at 13.80° N and 75.30° E about 30 km southwest of Shimoga town. Seismicity in this region is only sporadic with no past records of any earthquake activity. This earthquake comprises regions of northern Karnataka and the western most parts of Andhra Pradesh covering major cities like Mehboobnagar, Adoni, and Dharmavaram of Andhra Pradesh and Bijapur, Raichur, Bellary, Shimoga, Chitradurga, and Hassan of Karnataka. Some of its main tributaries include Bhima, Tungabhadra, Dharma, Kumudavati, Hemavati, and Hagari and the Penna River and its tributaries drained the nearby area.

4.8. Killari Earthquake

Killari earthquake, also known as the Latur earthquake, struck on September 30, 1993, with the main shock having a moment magnitude of 6.1 and focal depth of 5 km. The epicenter of the earthquake was located at 17.98° N and 76.46° E. The sheet includes the Upper Godavari Valley, Tapti Valley, and Plateau Terrains with more than 90% of the area covered by Deccan trap. This was an intraplate earthquake having major faults and lineaments that trend towards Northwest and Southwest of the area and covered by Deccan trap and East-West that is parallel to the Saptura trend, in the extreme north. The epicenter of the earthquake was located to be near the intersection of Northwest Southeast and East-north-east and West-south-west trending faults.

4.9. Jabalpur Earthquake

Jabalpur earthquake struck on December 22, 1997 with a moment magnitude of 5.8 and focal depth of 36 km. The epicenter was located at 23.11° N and 80.07° E. The isoseismic map constituted of major portion of Madhya Pradesh, parts of Uttar Pradesh and Maharashtra including some of the major cities like Bina, Nagpur, Chhindwara, Blaghat, Bhandara, and Tikamargh. Narmada and Tapti form the major drainage system. The fault area is covered by a layer of basalt flows (about 4 m thick at Jabalpur) with basal contact of the Lameta rock at ground surface at many locations. The soil in the area is known as “black cotton soil”; it is black or dark grey and contains a high percentage of montmorillonite. This soil has very high compressibility and shrinkage, and very high swelling characteristics, which might be responsible for larger damage due to this moderate earthquake.

4.10. Pala Earthquake

The main shock was on December 12, 2000 and was located 5–6 km southwest of Eratupetta. The epicentre of this earthquake is at 9.71° N and 76.88° E, which is aligned more or less in a north-south direction passing through Melukavu and Eratupetta, with majority of the events having focal depths less than 12 km. This was felt widely in Kerala and adjoining parts of Tamil Nadu. Cracks appeared in some houses in the epicentre area. A few buildings in Melukavu region developed cracks and some open wells went dry in Kanjirappally area after this earthquake.

4.11. Bhuj Earthquake

The Bhuj earthquake occurred on January 26, 2001, which is India's 51st Republic day and lasted for about 2 min. The moment magnitude of the earthquake was 7.6 with a focal depth of 25 km. The epicenter was located at 23.4° N and 70.3° E, about 9 km south-southwest of the village Chobari in Bhachau Taluka of Kutch District of Gujarat, India. The earthquake reached a magnitude of between 7.6 and 7.7 on the moment magnitude scale and had a maximum felt intensity of 'X' on the Mercalli Intensity Scale. The quake killed around 20,000 people, injured another 1,67,000, and destroyed nearly 4,00,000 houses. The most affected cities were Bhachau, Bhuj, Anjar, Rapar, Gandhidham, and Kandla city of Kutch district. The Kutch area falls in the highest seismic zone (Zone V) in the seismic zoning map of India.

Even though the above discussion shows the extent of damage distribution and continuous threat of earthquake in many parts of PI, limited studies are carried out to list and rank best suitable ground motion prediction equations for seismic hazard analysis. In this study, efficacy test has been carried out considering above past earthquakes and identified suitable GMPEs for PI for different distance segment.

5. Ground-Motion Prediction Equations Applicable for PI

Most of the stable continental regions in the world have poor strong-motion data and are not representative of the existing seismic hazard in the region [Menon *et al.*, 2010]. For the area having poor seismic record, the alternative is to develop synthetic ground-motion models. Regional synthetic ground-motion model should include seismotectonic and geological settings (e.g., shallow crustal intraplate earthquakes) in the region. Even though India is experiencing several earthquakes however, development of region specific GMPE models is limited [Anbazhagan *et al.*, 2012]. Region-specific GMPEs are countable and inadequate for many parts of India. Seismic hazard studies and GMPEs considered with assumed weights are summarized in Table 2. It can be noted from table that many studies used the GMPEs that are not applicable for PI and considered multiple GMPEs with equal weights. PI has two region specific GMPEs developed by Raghukanth and Iyengar [2007] and NDMA [2010]. In this study, the existing GMPEs developed for different tectonic environments similar to PI and GMPEs developed for regional hazard studies are also considered. Three regionally developed GMPEs for peninsular India and eight GMPEs developed for other intraplate regions are available for seismic hazard analysis in the region. The models developed in Eastern North America (ENA) are applicable to the intraplate regions of India because of the similarity in regional tectonics [Bodin *et al.* 2004]. Raghukanth and Iyengar [2007] observed that their model for India has ground-motion predictions similar to the available models for other intraplate regions. Schweig *et al.* [2003] discussed the similar features shared by ENA and PI in terms of observed seismogenic

TABLE 3 List and abbreviations of the GMPEs

Sl. No.	Attenuation Equation	Abbreviation of the Equation
1	Hwang and Huo [1997]	HAHO-97
2	Toro *et al.* [2002], extension of Toro *et al.* [1997]	TOR-02
3	Kenneth W. Campbell [2003]	CAM-03
4	Behrooz Tavakoli and Shahram Pezeshk [2005]	TAPE-05
5	Gail M. Atkinson and David M. Boore [2006]	ATKB-06
6	Raghukanth and Iyangar [2007] – Respective region	RAIY-07
7	Raghukanth and Iyangar [2007] for Peninsular India	RAIY-07[PI]
8	Atkinson [2008], modification of Boore and Atkinson [2008]	ATK-08
9	The National Disaster Management Authority, Govt. of India, New Delhi [2010]	NDMA-10
10	Atkinson and Boore[2011], modification of Boore and Atkinson [2008]	ATKB-11
11	Pezeshk, *et al.*, [2011]	PEZA-11

activities and known seismotectonics. Based on the results of ground-motion attenuation analysis of the 2001 Bhuj earthquake, Cramer and Kumar [2003] suggested that the ground motion attenuation in ENA and PI is comparable. GMPEs applicable for peninsular India or Intraplate region are listed in Table 3. The functional forms of the equations, constant for peak ground acceleration (PGA) and range of magnitude and distance are given in Table 4. The above can be summarized as follows.

Hwang and Huo [1997] developed the GMPE to predict the PGA and spectral acceleration (SA) for rock and soil sites in the central and eastern United States. The authors simulated the bedrock ground motion for 56 pairs of moment magnitude M_w and epicentral distance R. For different possible combination of M_w and R, 550 samples of ground motion parameters were generated using a seismological model together with random vibration theory and distribution of extreme values. With the help of appropriate site coefficients, the GMPEs have been modified the rock site to soil site as per the site categories specified in the 1994 National Earthquake Hazard Reduction Programme (NEHRP). It has concluded that the ground motion simulated in their study is for far-field condition; thus, the attenuation relations established in the study are appropriate for the assessment of seismic hazards at far-field rock and soil sites in the Central Eastern United States [Hwang and Huo, 1997]. This GMPE HAHO-97 is valid for distance range of 5–200 km and moment magnitude range of 5–7.5. HAHO-97 GMPE and respective coefficients for bedrock condition are given in Table 4.

Toro *et al.* [1997] derived four sets of ground-motion attenuation equations for rock site conditions in central and eastern North America (CENA) based on the stochastic ground motion model of path effects by considering multiple rays in a horizontally layered model of the crust. The model and the values of their parameters were developed by an extensive analysis of ground-motion data. The amplification variation factor to calculate ground motion for soil sites is also provided in this study. The study concluded that the uncertainty

TABLE 4 Functional forms and validity of GMPEs considered in the study

Sl. No	Abbreviation of the GMPE	Functional form of the equation [peak ground acceleration in g]	Constants		Validity		Remarks
					Magnitude Range [M_W]	Distance Range [km]	
1	HAHO-97	$\ln(Y_{BR}) = C_1 + C_2M + C_3\ln[\sqrt{R^2 + H^2} + R_0(M)] + C_4\sqrt{R^2 + H^2} + \in$ $R_0[M] = 0.06\exp[0.7M]$ M-moment magnitude, R- Epicentral distance [km] and H- Focal Depth [km]	C_1	-2.904	5.0-7.5	5-200 [Depth 6-15]	GMPE is appropriate for seismic hazard assessment at far-field rock [3.5 km/s].
			C_2	0.926			
			C_3	-1.271			
			C_4	-0.00302			
			$\sigma_{\ln[YBR]}$	0.309			
2	TOR-02	$\ln Y = C_1 + C_2(M-6) + C_3(M-6)^2 - C_4\ln R_M - (C_5 - C_4)\max\left[\ln\left(\frac{R_M}{100}\right), 0\right] - C_6R_M + \varepsilon_e + \varepsilon_a$ Extended-source effects Approach [1] $R_M = \sqrt{R^2 + C_7{}^2[exp(-1.25 + 0.227M)]^2}$ M is moment magnitude, R is the closest horizontal distance to the rupture [km] Approach [2] $R_M = R_f + 0.06\exp[m_{blg}]$ For attenuation equations in terms of m_{blg} or $R_M = R_f + 0.089\exp[0.6M]$ for attenuation equations in terms of moment magnitude. In the above two equations, R_f is the shortest [slant] distanceto the fault rupture.	C_1	2.20	5.0-8.0	1-500	Extended-source effect has been introduced in order to account for large magnitudes and short distances. Applicable to hard rock [defined as having average shear-wave velocities of 6,000 ft/s at the surface]
			C_2	0.81			
			C_3	0.00			
			C_4	1.27			
			C_5	1.16			
			C_6	0.0021			
			C_7	9.3			
3	CAM-03	$\ln Y = c_1 + f_1(M_w) + f_2(M_w, r_{rup}) + f_3(r_{rup})$ $f_1(M_w) = c_2M_w + c_3(8.5 - M_w)^2$ $f_2(M_w, r_{rup}) = c_4\ln R + (c_5 + c_6M_w)r_{rup}$ $R = \sqrt{r_{rup}{}^2 + [c_7\,exp(c_8M_w)]^2}$ $f_3(r_{rup}) = \begin{cases} 0 & for\ r_{rup} \le r_1 \\ c_9(\ln r_{rup} - \ln r_1) & for\ r_1 < r_{rup} \le r_2 \\ c_9(\ln r_{rup} - \ln r_1) + c_{10}(\ln r_{rup} - \ln r_2)\ for\ r_{rup} > r_2 \end{cases}$	c_1	0.0305	5.0-8.2	r_{rup} = 1-1000	PGA was assumed to represent the value of PSA at 0.01-sec period. Hard rock with a shear-wave velocity of 2800 m/sec Appropriate for estimating hazard on
			c_2	0.633			
			c_3	-0.0427			
			c_4	-1.591			
			c_5	-0.00428			
			c_6	0.000483			

(*Continued*)

TABLE 4 (Continued)

		$r_{rup}$is closest distance to fault rupture $r_1 = 70\ km\ and\ r_2 = 130\ km$	c_7	0.683			hard rock for $M_w \geq 5.0$ and $r_{rup} \leq 70$ km. It has been extended for larger distances using stochastic ground-motion estimates.
			c_8	0.416			
			c_9	1.140			
		Aleatory standard deviation of ground motion are given by $\sigma_{lnY} = \begin{cases} c_{11} + c_{12}M_W & for\ M_W < M_1 \\ c_{13} & for\ M_W \geq M_1 \end{cases}$ Where M_1 =7.16	c_{10}	-0.873			
			c_{11}	1.030			
			c_{12}	-0.0860			
			c_{13}	0.414			
4	TAPE-05	$\ln(Y) = f_1(M_w) + f_2(r_{\text{rup}}) + f_3(M_w, r_{\text{rup}})$ $f_1(M_w) = C_1 + C_2(M_w) + C_3(8.5 - M_w)^{2.5}$ $f_2(r_{rup})$ $= \begin{cases} C_9 \ln(r_{\text{rup}} + 4.5) r_{\text{rup}} \leq 70\ \text{km} \\ C_{10} \ln\left(\frac{r_{\text{rup}}}{70}\right) + C_9 \ln(r_{\text{rup}} + 4.5) \quad 70 < r_{\text{rup}} \leq 130\ km \\ C_{11} \ln\left(\frac{r_{\text{rup}}}{130}\right) + C_{10} \ln\left(\frac{r_{\text{rup}}}{70}\right) + C_9 \ln(r_{\text{rup}} + 4.5) r_{\text{rup}} \geq 130\ km \end{cases}$ $f_3(M_w, r_{\text{rup}}) = (C_4 + C_{13}M_w) \ln R + (C_8 + C_{12}M_w)R$ $R = \sqrt{{r_{\text{rup}}}^2 + [C_5 \exp[C_6 M_w + C_7(8.5 - M_w)^{2.5}]]^2}$ r_{rup} is defined as the closest distance to the fault rupture[km] The aleatory standard deviation of $\ln Y$ is defined as a function of earthquake magnitude and is modelled as follows: $\sigma_{lnY} = \begin{cases} c_{14} + c_{15}M_W & M_W < 7.2 \\ c_{16}M_W \geq 7.2 \end{cases}$	C_1	1.14	5.0-8.2	Upto 1000	GMPE and finite source relationships predict equal ground-motion amplitude at low frequencies and near-source distances, but for large [$M_w \geq 6.4$] earthquakes at distances>100km the results estimate larges amplitudes. Boore[2000] suggestedρ_s = 2.8 g/cm^3 and β_s =3.6 km/sec for ENAwere used in this study as input to the stochastic simulation models
			C_2	0.623			
			C_3	-0.0483			
			C_4	-1.81			
			C_5	-0.652			
			C_6	0.446			
			C_7	-0.0000293			
			C_8	-0.00405			
			C_9	0.00946			
			C_{10}	1.41			
			C_{11}	-0.961			
			C_{12}	0.000432			
			C_{13}	0.000133			
			C_{14}	1.21			
			C_{15}	-0.111			
			C_{16}	0.409			
5	ATKB-06	$\text{Log}\, PSA = c_1 + c_2 M + c_3 M^2 + (c_4 + c_5 M) f_1 + (c_6 + c_7 M) f_2 + (c_8 + c_9 M) f_0 + c_{10} R_{\text{cd}} + S$ M is moment magnitude M and R_{cd} is closest distance to the fault	c_1	0.907	4.0-8.0	Upto 1000	Hard-rock sites [with shear-wave velocity ≥2 km/sec] in the northeastern United States and southeastern Canada
			c_2	0.983			
			c_3	-0.0660			
			c_4	-2.70			

(*Continued*)

TABLE 4 (Continued)

		$f_0 = max\left(\log\left(\frac{R_0}{R_{cd}}\right), 0\right)$ $f_1 = min(\log R_{cd}, \log R_1)$ $f_2 = Max\left(\log\left(\frac{R_{cd}}{R_2}\right), 0\right)$ $R_0 = 10,\ R_1 = 70,\ R_2 = 140$ and S =0 for hard-rock sites	c_5	0.159					The equation may over predict the near-source ground motion, if there are significant saturation effects that are not accounted for in the simulation model.
			c_6	-2.80					
			c_7	0.212					
			c_8	-0.301					
			c_9	-0.0653					
			c_{10}	-0.000448					
6 & 7	RAIY-07	$\ln(y_{br}) = c_1 + c_2(M-6) + c_3(M-6)^2 - \ln[r] - c_4 r + \ln[\varepsilon_{br}]$ $y_{br} = \frac{S_a}{g}$ M is Moment magnitude and r is hypocentral distance Note: 1- Peninsular India, 2- Koynawarna, 3- South India, 4- Western Central India.		1	2	3	4	5.0-8.0	30-300	The results are valid at bedrock level with V_S=3.6 km/s. For other site conditions equation is to be modified using site factors
			c_1	1.6858	1.7615	1.7816	1.7236		
			c_2	0.9241	0.9325	0.9205	0.9453		
			c_3	-0.0760	-0.0706	-0.0673	-0.0725		
			c_4	0.0057	0.0086	0.0035	0.0064		
8	ATK-08	$Y_{ENA} = FY_{BA08}$ $\log F = c_0 + c_1 R_{jb} + c_2 R_{jb}{}^2$ M is moment magnitude and $R_{JB\ is}$ closest horizontal distance to the surface projection of the fault plane $[Y_{BA08}]\quad \ln Y = F_M(M) + F_D(R_{JB}, M) + F_s(V_{S30}, R_{JB}, M) + \varepsilon\sigma_T$ $F_D(R_{JB}, M) = [c_1 + c_2[M - M_{ref}]]\ln(R/R_{ref}) + c_3(R - R_{ref})$ For M≤ M_h, $F_M(M) = e_1 U + e_2 SS + e_3 NS + e_4 RS + e_5(M - M_h) + e_6(M - M_h)^2$ For M >M_h, $F_M(M) = e_1 U + e_2 SS + e_3 NS + e_4 RS + e_7(M - M_h)$ $U = 1, SS = 0, NS = 0, RS = 0$ for unspecified fault – type $M_{ref} = 4.5,\quad R_{ref} = 1\ km$ $F_s = F_{LIN} + F_{NL}$ $R = \sqrt{R_{JB}^2 + h^2 F_{LIN}} = F_{NL} = F_s = 0$ $R = \sqrt{R_{JB}^2 + h^2}$	c_0	0.287			5.0-8.0	R_{JB}<200	Uncertainty in median ENA GMPEs is afactor of 1.5–2 for M ≥5 at distances from 10 to 70 km. Uncertaintyis greater than a factor of 2 for large events [M ≥7]at distances within 10 km of the source.
			c_1	0.0012					
			c_2	0.0000023					
			c_1	-0.66050					
			c_2	0.11970					
			c_3	-0.01151					
			h	2.54					
			e_1	-0.53804					
			e_2	-0.50350					
			e_3	-0.75472					
			e_4	-0.50970					
			e_5	0.28805					
			e_6	-0.10164					
			e_7	0.0000					
			M_h	6.75					
9	NDMA-10	$\ln\left(\frac{S_a}{g}\right) = C_1 + C_2 M + C_3 M^2 + C_4 r + C_5 \ln(r + C_6 e^{C_7 M}) + C_8 \log(r)\, f_0 + \ln[\in]$ $f_0 = max(ln(r/100), 0)$ Sa is the spectral acceleration, M is the moment magnitude, r is the hypocentral distance in kilometers		1	2	3	4.0-8.5	1-500	These results can be used to construct the mean and [mean+sigma] response spectrum on A-type rock in any part of India.
			C_1	-5.2182	-3.7671	-4.7653			
			C_2	1.6543	1.2303	1.3935			
			C_3	-0.0309	-0.0019	-0.0162			
			C_4	-0.0029	-0.0027	-0.0020			

(*Continued*)

TABLE 4 (Continued)

		Note:1- Peninsular India, 2- Central India, 3- Gujarat region.	C_5	-1.4428	-1.4857	-1.4183		
			C_6	0.0188	0.0385	0.0187		
			C_7	0.9968	0.8975	0.9899		
			C_8	0.1237	0.1301	0.1243		
10	ATKB-11	$Y'_{ENA} = YF_{BA08}F_{ENA}$ $\log F_{ENA} = c(T) + d[T]R_{jb}$ $\log F_{BA08} = \max(0, 3.888 - 0.674M)$ $- \max(0, 2.933 - 0.510M)\log[R_{jb} + 10]$	*c[T]*	0.419				The GMPEs are in good agreement with the ground-motion data for moderate-magnitude events.
			d[T]	0.00211				
			Y	Y_{BA08}				
11	PEZA-11	$\log(\overline{Y}) = c_1 + c_2M_w + c_3{M_w}^2 + (c_4 + c_5M_w)\min\{\log(R), \log(70)\} + (c_6 + c_7M_w)\max[\min\left\{\log\left(\frac{R}{70}\right), \log[\frac{140}{70}]\right\}, o] + (c_8 + c_9M_w)\max\left\{\log\left(\frac{R}{140}\right), 0\right\} + c_{10}R$ Where $R = \sqrt{{R_{rup}}^2 + {c_{11}}^2}$ $\overline{Y}$ is the median value of PGA or PSA [g], M_w is the moment magnitude and R_{rup} is the closest distance to fault rupture [km] The mean aleatory standard deviation of $\log(\overline{Y})$ is modeled as follows: $\sigma_{\log \overline{Y}} = \begin{cases} c_{12}M_w + c_{13} & M \le 7 \\ -6.95 \times 10^{-3}M_w + c_{14} & M > 7 \end{cases}$	c_1	1.5828			5.0 – 8.0	R_{rup} up to 1000 km	GMPE underpredicts the observations at close distances [upto 60 km]. There is a good agreement between the ground-motion predictions of this equation and the ENA database at large distances [$R_{rup} \ge 200$ km].
			c_2	0.2298				
			c_3	-0.03847				
			c_4	-3.8325				
			c_5	0.3535				
			c_6	0.3321				
			c_7	-0.09165				
			c_8	-2.5517				
			c_9	0.1831				
			c_{10}	-0.0004224				
			c_{11}	6.6521				
			c_{12}	-0.02105				
			c_{13}	0.3778				
			c_{14}	0.2791				

computed for rock sites is an upper bound for the uncertainty for soil sites provided it belongs to same category. Toro [2002] modified the Toro *et al.* [1997] attenuation equations for larger magnitudes and short distances considering empirical modeling approach by introducing the extended-source effects. The epistemic uncertainty is treated as magnitude dependent and is modeled in the seismic-hazard calculations by using four separate attenuation equations and their associated weights. TOR-02 [Toro, 2002] GMPE is given in Table 4 and is valid for up to distance of 500 km and moment magnitude range of 5–8.0.

Campbell [2003] proposed a hybrid empirical method that uses the ratio of stochastic or theoretical ground motion to adjust the empirical ground-motion relations developed for one region to another region. Campbell [2003] presented a formal mathematical framework for the hybrid empirical method and applied it to the development of ground-motion relations for PGA and spectral acceleration (SA) in ENA using empirical relations from Western North America (WNA). The hybrid empirical ground-motion relations developed in this manner was considered to be the most appropriate for estimating ground motion for earthquakes of $M_w \geq 5.0$ and rupture distance (r_{rup}) ≤ 70 km. It was extended to a larger distance using stochastic ground-motion estimates, so that it can be used in more general engineering applications. The resulting ENA ground-motion relation is valid for estimating ground motions for hard-rock site (shear-wave velocity of 2800 m/s) and for earthquakes of M_w 5.0–8.2 and fault rupture distances (r_{rup}) of 0–1000 km.

Tavakoli and Pezeshk [2005] utilized an alternative approach based on a hybrid-empirical model to predict the ground-motion relationship for ENA. A stochastic model was first used to derive modification factors from the ground motions in WNA (Western North America) to the ground motions in ENA. Authors developed an empirical-stochastic source model for the region to obtain ground motions at different magnitude–distance range of interest. A point source model was used to consider the effect of finite-fault modelling on the ground-motion parameters. The empirical-stochastic GMPE for horizontal PGA and SA developed is applicable to earthquakes of M_w 5.0–8.2 at hypocentral distances of up to 1000 km.

Atkinson and Boore [2006] developed the ground-motion prediction equation for hard-rock condition and soil sites in ENA, including estimation of the aleatory uncertainty (variability) based on a stochastic finite-fault model. The model incorporates the new information obtained from ENA seismographic data gathered from 1995–2005, including three-component broadband data that provide new information on ENA source and path effects. These prediction equations are similar to the ground-motion prediction equations of Atkinson and Boore [1995], which were based on a stochastic point-source model. The prediction equations matches well with the available ENA ground-motion data as evidenced by near-zero average residuals (within a factor of 1.2) for all frequencies, and the lack of any significant residual trends with distance.

Iyengar and Raghukanth [2004] and Raghukanth and Iyengar [2007] statistically simulated ground motions for peninsular India using a well-known stochastic seismological model and regional seismotectonic parameters. Iyengar and Raghukanth [2004] presented GMPE to estimate only PGA, whereas Raghukanth and Iyengar [2007] presented an empirical relation for estimating 5% damped response spectra, as a function of magnitude and source-to-site distance covering bed rock and soil site conditions. These relations were validated by comparing the PGA from instrumented data of two strong earthquakes in Peninsular India namely Koyna (December 11, 1967) and Bhuj (January 26, 2001). Authors divided PI as three regions based on quality factor (Q) and developed GMPE for each region separately and combined one. Figure 3 shows earthquake locations with boundaries of these three regions as per Iyengar and Raghukanth [2004] and Raghukanth and Iyengar

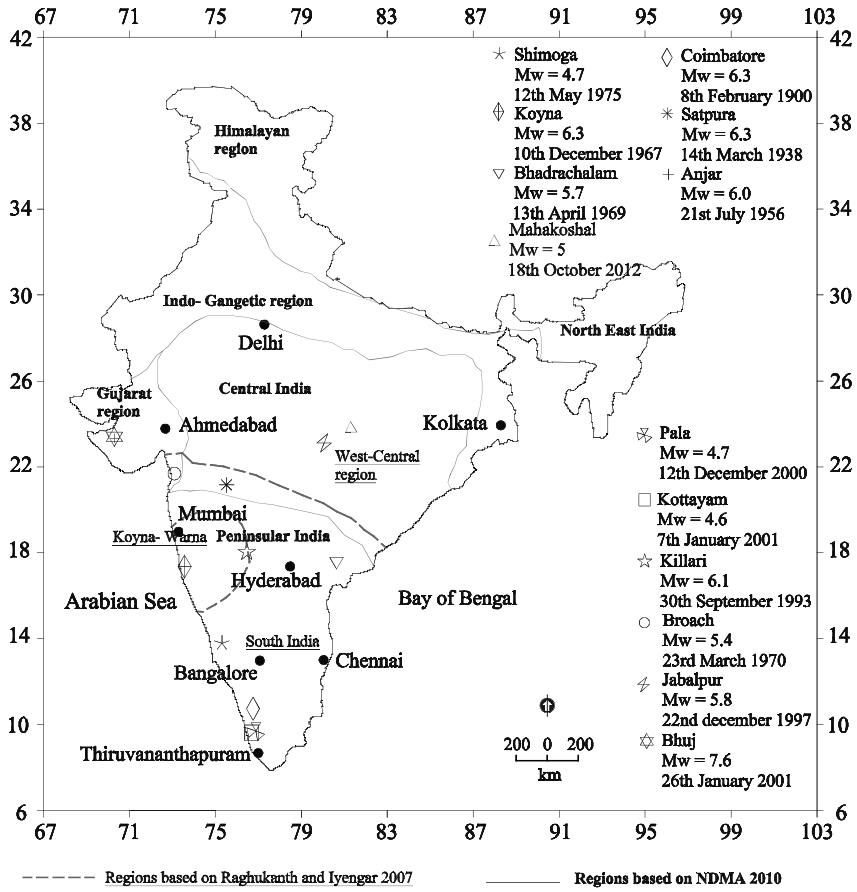

FIGURE 3 Regional sub classification of PI for GMPE development with past earthquake locations.

[2007]. Separate coefficients were given for each of these regions along with the entire Peninsular India GMPE. In this study, GMPE applicable to each region [RAIY-07] and GMPE for PI [RAIY-07(PI)] has been used in the ranking system, therefore eleven GMPEs are considered in this study.

Atkinson [2008] followed a referred empirical approach to develop GMPEs for ENA. This approach combines the ENA ground-motion database with the empirical prediction equations of Atkinson and Boore [2006] for the reference region of WNA. The author has provided an alternative model that helps to define epistemic uncertainty rather than replacing the AB06 equation. In this referred empirical approach, the author used a stochastic model and other seismological model to develop the regional adjustment factors unlike the hybrid empirical approach. The differences between the referred empirical GMPE and the stochastic GMPE of Atkinson and Boore [2006] were also discussed. Inconsistencies between both of the studies led to the conclusion that the uncertainty in median ENA GMPEs is about a factor of 1.5–2 for $M_w \geq 5$ at distances from 10–70 km. Uncertainty has been found to be greater than a factor of 2 for large events ($M_w \geq 7$) at distances within 10 km of the source.

Finite fault stochastic seismological model has been used by NDMA [2010] to develop strong motion attenuation relations for seven geological provinces of India with different

stress drops and quality factors. The seven regions considered by them are the Himalayas, the Indo-Gangetic region, the Peninsular India, the Northeast India, Gujarat, Central India and Andaman-Nicobar. Study area region considered in this study consist of PI, Gujarat region, and part of Central India. Geological provinces marked by NDMA [2010] are shown in Fig 3. The GMPEs proposed by NDMA [2010] are compared with the instrumental PGA values from the respective region geological provinces. These equations are used to generate probabilistic seismic hazard map of India and presented PGA and SA for different return period at bedrock.

Atkinson and Boore [2011] compared the GMPEs of western North America [Boore *et al.*, 2008] and eastern North America [Atkinson and Boore, 2006; Boore *et al.*, 2008] to newly available ground-motion data and they revised both region GMPEs. The revised GMPE for ENA affect all magnitudes. Simple modifications to the existing GMPEs make them significantly better and in agreement with the actual data. Authors recommend the use of updated GMPEs for seismic hazard analyses and other applications.

Pezeshk *et al.* [2011] developed a new GMPE for ENA hard-rock site with $V_S^{30} \geq 2000$ m/s (NEHRP site class A). The new GMPE is applicable for a magnitude range of 5–8 and closest distances to the fault rupture up to 1000 km was derived. The GMPE was developed using stochastic simulation method for the response spectra (pseudo acceleration for 5% damping) and the PGA hard-rock sites in ENA. A median hybrid empirical estimates was obtained for ENA ground motion by scaling the WNA empirical relations using theoretical modification factors. The limitation of hybrid empirical method is that it only provides a reliable estimates out to 70 km. To avoid this, a method proposed by Campbell [2003] was used. This method scales the stochastic ENA ground-motion prediction by the factor required to make its estimate at $R_{rup} = 70$ km equal to the hybrid method prediction. These scaled estimates were used as estimates for R_{rup} beyond 70 km in regression process (to 1000 km) to develop GMPEs. For site conditions other than site A, the predictions must be modified using an appropriate method.

It can be noted from above review that most of GMPEs are applicable for magnitudes (Mw) range of 4–8 and hypocentral distance of 1–1000 km. In order to compare these GMPEs, magnitude M_w of 6 has been considered and PGA is estimated up to a hypocentral distance of 500 km. Figure 5 shows comparison of applicable GMPEs for PI. It can be observed from Fig 5 that all the curves follow a similar pattern and few curves give a higher range of PGA values.

6. Selection of GMPES

Eleven GMPEs are applicable for any part of PI, of these eight were developed elsewhere for similar seismotectonic provinces. Simple GMPEs involves magnitude and distance parameters, whereas complicated ones need fault rupture parameters in addition to faulting types and site attributes to determine the peak ground-motion [Nath and Thingbaijam, 2011]. Developments of GMPEs are found to be consistent after the year 2000 as opposed to the developments before 2000. Increasing number of GMPEs for seismic hazard assessment necessitates an efficient, quantitative, and robust method to select and rank these models for a particular region of interest [Delavaud *et al.*, 2009]. Proper selection of GMPEs is significant in predicting the level of ground shaking and it is a key element in any seismic hazard analysis [Bommer *et al.*, 2010]. GMPEs development over the past four decades have shown consistency in associated variability and epistemic uncertainty and thereby increasing complexities [Nath and Thingbaijam, 2011; Strasser *et al.*, 2009; Douglas, 2010]. This necessitates the usage of multiple GMPEs in a logic tree framework for the hazard analysis and consequently the selection and ranking of GMPEs [Cotton *et al.*,

2006; Nath and Thingbaijam, 2011; Bommer *et al.*, 2005; Sabetta *et al.*, 2005; Scherbaum *et al.*, 2004, 2005; Hintersberger *et al.*, 2007].

Selection of GMPEs can be carried out using the criteria suggested by Bommer *et al.* [2010] and also by efficacy tests proposed by Scherbaum *et al.* [2009]. Efficacy test can be performed for a quantitative assessment of GMPEs for a particular region. This will provide a ranking order for a set of GMPEs towards appropriate selection based on observed earthquakes in the region. In the present study, the information-theoretic approach proposed by Scherbaum *et al.* [2009] has been used. The efficacy test makes use of average sample log-likelihood (LLH) method for the ranking purpose and was successfully performed by Delavaud *et al.* [2009] and further applied by Nath and Thingbaijam [2011] for the whole Indian subcontinent. Nath and Thingbaijam [2011] gave a list of GMPEs for Himalayas, Northeast India, and Peninsular India considering few GMPEs and past earthquakes. The authors have not included the recent GMPEs proposed by NDMA-10, ATKB-11, and PEZA-11 and considered very few earthquake Isoseismal values for entire PI. In order to quantify the suitability of GMPEs, ranking estimator, i.e., average LLH values has been calculated for all the GMPEs, which gives a ranking order for the set of equations considered.

In this study efficacy test has been carried out by considering the past damaging earthquakes reported in PI and the relation between the PGA and European Macroseismic Scale [Grünthal, 1998] at rock sites given by Nath and Thingbaijam [2011]. As a first step towards ranking, PGA values were estimated for the occurred earthquake magnitudes using all GMPEs (see Table 4). The earthquake recording data i.e. time history across the PI do not consist of enough data to maintain an efficient judgment. So, PGA values calculated considering all the applicable GMPEs are converted to EMS using relation between PGA and EMS (using Eq. (1)) proposed by Nath and Thingbaijam [2011] as it is the only available conversion applicable to India:

$$EMS = 4.49 + 2.42log_{10}\,(PGA) + 1.35log_{10}\,(R)\,. \tag{1}$$

To derive the above equation a nonlinear regression analysis is performed between the observed PGA and EMS which also considers hypocentral distance (R), magnitude, and intensity from the 33 recorded data sets [Nath and Thingbaijam, 2011]. The authors highlighted that the uncertainty in the conversion from predicted PGA to EMS is considerably less as compared to other similar relations. This derived equation exhibits less dispersion, while calculating the residual between observed and calculated EMS intensity values. This clearly shows that the uncertainty in the conversion from predicted PGA to European Micro-Seismic Scale (an intensity measure) is considerably less, which may not affect the ranking of GMPEs and further its weight calculation. Due to employment of distance term in the equation, the standard deviation in prediction of EMS value is lower. Despite having a semi-quantitative nature, intensities play a vital role where there is a lack strong motion database and stations. Moreover, this is the only available equation for the Indian subcontinent and secondly as the recorded time history data is very less for PI, in this study, PGA calculated from various GMPEs is converted to EMS using that particular equation (equation 1). Presently, uncertainty associated in the conversion also reflects in the calculation of weights and if large numbers of earthquake acceleration histories are available for the region, then GMPEs can be directly ranked based on measured data.

To derive the ranking criteria of GMPE, Kullback-Leibler (KL) distance was used. The KL divergence scale between two models f and g has been defined as

$$D(f,g) = E_f\left[log_2(f)\right] - E_f\left[log_2(g)\right], \tag{2}$$

where E_f is the statistical expectation taken with respect to model f.

The KL distance denotes the information loss when a model (f) defined as a distribution is used to approximate a reference model (g). If model f represents nature than it cannot be calculated. However, to compare the two models as g_1 and g_2, only their relative KL distance is estimated, i.e., $D(f,g_1) - D(f,g_2)$, whereas the unknown model f drops out to be constant. However, to calculate the LLH value between the two models, these models are assumed as two continuous probability distribution functions. The KL divergence between two models is represented by their probability density functions. As the reference model represents the data generation process and can be acknowledged only through observations, the self-information of that model cannot be calculated. So, LLH is approximated using the equation proposed by Delavaud *et al.* [2009] and given in Eq. (3):

$$LLH(g,x) = -\frac{1}{n}\sum_{i=1}^{N} log_2(g(x_i)) \tag{3}$$

where, $x = \{x_i\}, i = 1, \ldots .N$ are the empirical data and $g(x_i)$ is the likelihood that model g has produced the observation x_i. In this case, g is the probability density function given by a GMPE to predict the observation produced by an earthquake with magnitude M at a site i that is located at a distance R from the source [Delavaud *et al.*, 2012]. The probability distribution of PGA value derived from eleven GMPEs considering a particular magnitude and varying hypocentral distance is used to determine the LLH values (using Eq. (3)). Furthermore, the average of the LLH with varying hypocentral distance has been taken and used for ranking of the GMPEs. Due to its negative sign, the negative average sample log-likelihood is not a measure of closeness but a measure of the distance between a model (using GMPE) and the data-generating process [Delavaud *et al.*, 2012]. To reduce the uncertainty, a large number of EMS points was used, which reduces the variance and hence converging the ranking order as derived using the PGA values [Delavaud *et al.*, 2009]. The comprehensive details about computation of LLH values is mentioned in Delavaud *et al.* [2009, 2012].

In order to highlight the performance of the GMPEs at different distance ranges, the entire distance has been broken into two segments of 0–200 km and 200 to the maximum damaged distance as given in Table 1, last column. The average LLH values for all the 11 equations for the appropriate distance segments have been calculated. LLH value estimates are used to rank GMPEs, i.e., lower LLH means higher rank for each earthquake in two-distance segment. These LLH values are further used to estimate LLH based weights considering Eq. (4) given in Delavaud *et al.* [2012a]. The LLH based weights tells us the degree to which data increase or decrease the weight of a model with respect to the state of non-informativeness [Delavaud *et al.*, 2012a,b].

LLH values and weights of all GMPEs are indicative of the order of GMPEs and closeness to the actual hazard value. LLH values are not a measure of closeness but a measure of the distance between a model and the data-generating process [Delavaud *et al.,* 2012a,b]. Delavaud *et al.* [2012b] gave a parameter called Data Support Index (DSI) to know the percentage by which the weight on a model is increased or decreased through data. DSI estimated from Eq. (5) shows the percentage increase or decrease of weight of a model with respect to its state of non-informativeness [Delavaud *et al.*, 2012b]:

$$w_i = \frac{2^{-LLH(g_i,x)}}{\sum_{k=1}^{n} 2^{-LLH(g_i,x)}} \tag{4}$$

$$DSI_i = 100\frac{w_i - w_{unif}}{w_{unif}} \tag{5}$$

where $w_{unif} = 1/M$ and M is the number of model used for calculation of LLH value, positive DSI value shows that the GMPE supports the observed model whereas a negative DSI rejects the model. Delavuad *et al.* [2012a] also stated that the difference in DSI value is an indicator of the ability of the model to predict the data. In the present study, DSI values are directly calculated using LLH and weights are calculated later for only those equations that are having a positive DSI. Table 5 shows typical calculation of LLH values, weights, and DSI for Coimbatore earthquake considering 11 GMPEs. Maximum distance of damage based on Isoseismal map, i.e., 500 km (Fig. 4 and Table 1) has been divided as 0–200 km and 200–500 km. LLH values vary from 1.619–3.925. It can be noted from Table 5 that LLH values and rank order at segment distance are different from the conventional 0–300 km (last two columns) values. It can be noted from Tables 4 and 5 that Nath and Thingbaijam [2011] has not included 4 GMPEs in their study and few GMPEs applicable up to 200 km are used in the 0–300 km ranking. Among all GMPEs, GMPE having positive DSI is considered for weight calculation and final recommendation with ranking order. More discussion about segmented distance and 0–300 km ranking is presented in the next section.

7. Results and Discussions

Ranking of GMPEs not only provides the best suitable GMPEs for the region but also helps in predicting the seismic hazard by reducing the epistemic uncertainty. In this study, GMPEs ranking for PI are presented considering all applicable GMPEs for the region and past earthquakes. For each earthquake, PGA values are estimated using all the applicable GMPEs and this has been converted to EMS value using the relation given by Nath and Thingbaijam [2011]. Calculated EMS values are compared with observed Intensity from the Isoseismal maps. Delavaud *et al.* [2009] highlighted the importance of macroseismic intensities values for selection of GMPE for region having poor recordings of past earthquakes. Delavaud *et al.* [2009] found that GMPE selection-based response spectra and macroseismic intensities lead to similar conclusions in terms of appropriateness of a GMPE model, although they do not carry the same information. Figure 6 shows calculated EMS from applicable GMPEs and observed EMS from Isoseismal map for Coimbatore Earthquake. It can be noticed in Fig. 6 that the calculated EMS values are lower than that of the observed intensities. This may be due to the fact that the equation given for converting PGA to EMS is at rock depth, whereas the observed intensities include the site effects and building damages. Similar observations are also noticed for other past earthquakes. The maximum distance to rank GMPEs is decided based on their respective Isoseismal maps. The maximum distance at which an intensity of 5–4 is experienced is taken as the maximum distance range for that particular earthquake. If this distance is less than 200 km then 0–200 km is considered as the maximum distance range. These rankings are compared with the rankings based on LLH calculated for the 0–300 km range given by Nath and Thingbaijam [2011].

Ranking based on LLH values for each distance segment are presented for past earthquakes in Figs. 7a–k. Figure 7 is the 3-D plot of rankings that shows all GMPE's ranking

TABLE 5 Typical calculation of Log-likelihood [LLH], LLH based weights [W] and Data support index [DSI]for Coimbatore earthquake using all GMPEs for different distance segments

	0–200 km				200–500 km				Nath and Thingbaijam [2011]* [0–300 km]	
GMPEs	LLH	DSI	W	Rank	LLH	DSI	W	Rank	LLH	Rank
HAHO-97	1.619	53.5363	0.195	1		NA			2.7369	4
TOR-02	2.193	3.4246	0.131	6	1.882	91.7751	0.319	2	2.5859	2
TAPE-05	2.608	−22.6978	NC	NR	4.912	−76.5214	NC	NR	2.8335	7
ATKB-06	3.488	−57.7043	NC	NR	2.154	59.0428	0.265	3	2.3939	1
CAM-03	1.985	19.6301	0.152	5	5.023	−78.2451	NC	NR	2.7810	6
RAIY-07	2.245	−0.0983	NC	NR	4.069	−57.9722	NC	NR	NC	
ATK-08	1.893	27.3306	0.161	4		NA			2.6911	3
RAIY-[PI]-07	1.621	53.5043	0.195	2	1.504	148.8741	0.415	1	2.7526	5
NDMA-10	1.872	29.1081	0.164	3	3.563	−40.1503	NC	NR	NC	
ATKB-11	3.925	−68.8224	NC	NR		NA			NC	
PEZA-11	2.907	−37.2112	NC	NR	3.731	−46.8031	NC	NR	NC	

Note: 1) NA: - Not Applicable and 2) NC: - Not considered and * Previous study in the region.

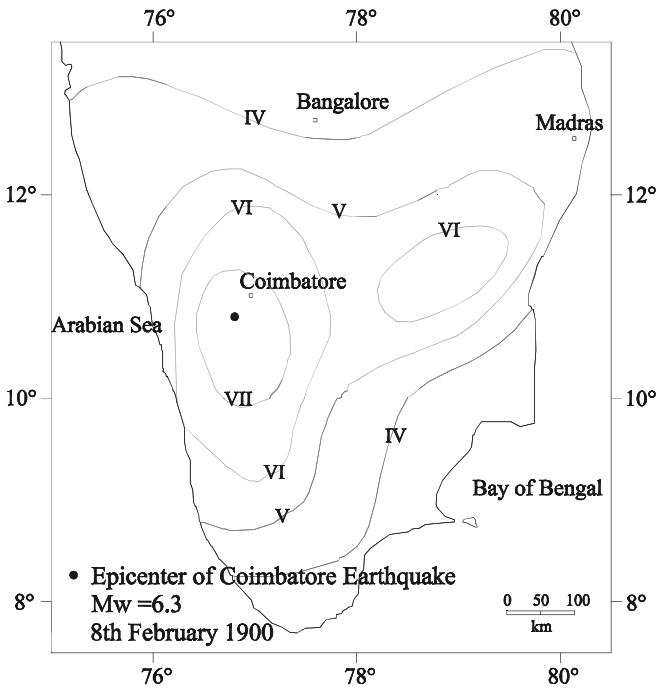

FIGURE 4 Isoseismic map of Coimbatore earthquake (modified after Anbazhagan *et al.*, 2012).

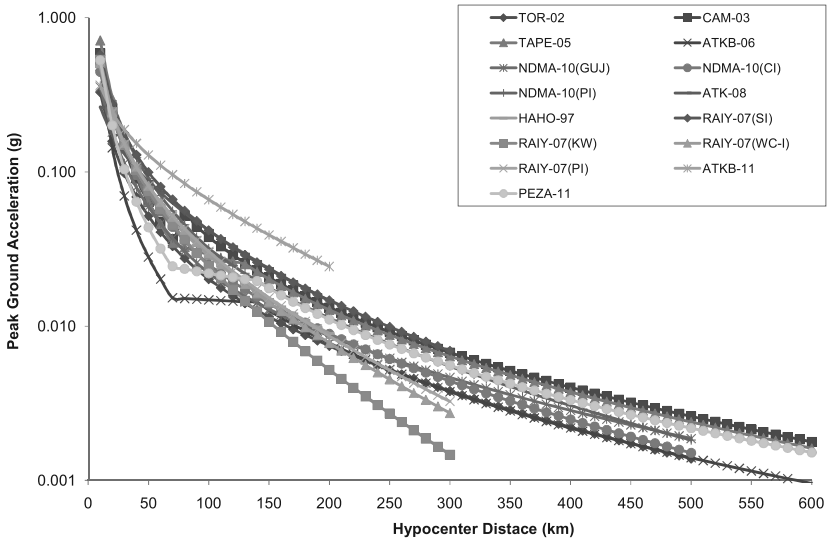

FIGURE 5 Comparison of applicable GMPEs of Peninsular India (for abbreviations refer to Fig. 3 and Table 3).

order for different distance segments. Here GMPEs not valid for a particular distance segment is marked in zero ranking level. Coimbatore earthquake ranking (Fig. 7a) is considered for the discussion. As per 0–300 km conventional rankings, ATKB-06 is ranked first, whereas segmented distance based ranking shows that ATKB-06 is ranked third for distance

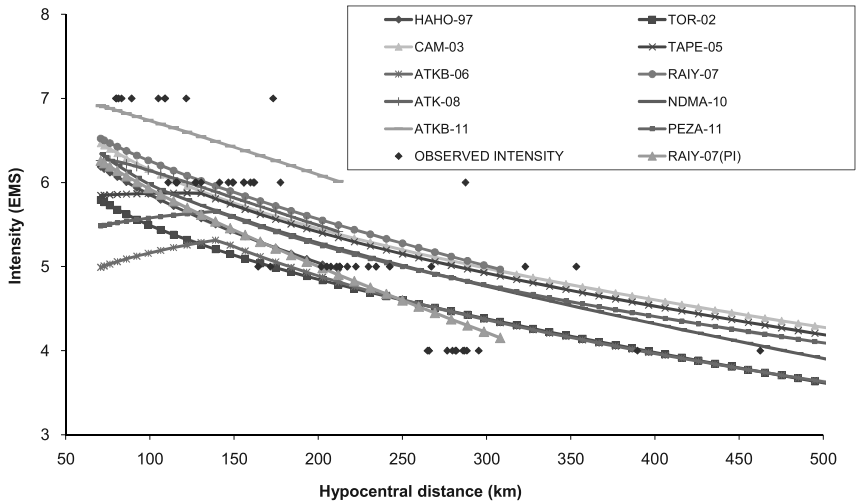

FIGURE 6 Comparison of EMS values estimated from applicable GMPEs and observed EMS reported in Isoseismal map (Fig. 2) for Coimbatore Earthquake.

200–500 km and is not surfaced in 0–200 km segment (Table 5). TOR-02 is ranked sixth in 0–200 km range and is ranked second in 200–500 km segment and 0–300 km ranking. ATK-08 is ranked fourth in 0–200 km segment and ranked third in 0–300 km ranking system, though it is not valid beyond 200 km. Similarly, HAHO-97 is ranked fourth in 0–300 km ranking but it is not valid beyond 200 km. However, it is ranked first for Coimbatore region for the distance segment of 0–200 km. Similarly, region specific GMPE of RAIY (PI)-07 is ranked fifth in 0–300 km ranking system, but it is ranked second in 0–200 km and first with lowest LLH value for 200–500 km in the segmented analysis. The top five-ranked GMPEs are recommended/used in seismic hazard analysis (SHA) and remaining GMPEs are discarded in 0–300 km system. CAM-03 is discarded in 0–300 ranking system but has surfaced as fifth position in segmented ranking for 0–200 km. RAIY-07 for south India, NDMA-10, ATKB-11, and PEZA-11 were not considered by Nath and Thingbaijam [2011] for 0–300 km ranking system. However, NDMA-10 is ranked third with DSI of 29.11 in the 0–200 km segment distance for Coimbatore region. From the above discussion, it is clear that segmented based region specific efficacy tests gives more reliable GMPE ranking based on regional data. Therefore, clubbing all GMPEs applicable to PI earthquakes and carrying efficacy test 0–300 km may not be appropriate.

Further, segmented distance ranking of GMPE is adopted for all past earthquakes in PI and results are presented in Fig. 7a–k. Figure 7 shows all GMPE ranking based on LLH values. In this study, only GMPE having positive DSI is considered for recommendation rather than taking top five. Because of this, the number of GMPEs applicable to each region for 0–200 km and 200–500 km are completely different from previous study by Nath and Thingbaijam [2011] 0–300 km ranking system. It can be noted that the efficacy test was not carried out for segment where data is insufficient. Each earthquake region was considered as two segments, efficacy test was as carried out, and DSI values were estimated using LLH values. For each distance segment, positive DSI values were identified and ranked based on maximum to minimum values. A maximum positive DSI value is considered as first rank and minimum is considered as lowest rank. Weights are estimated considering GMPEs having positive DSI values and which may be used for seismic hazard analysis in the region. Table 6 shows DSI for each segment, weights based on positive DSI, and final ranking of

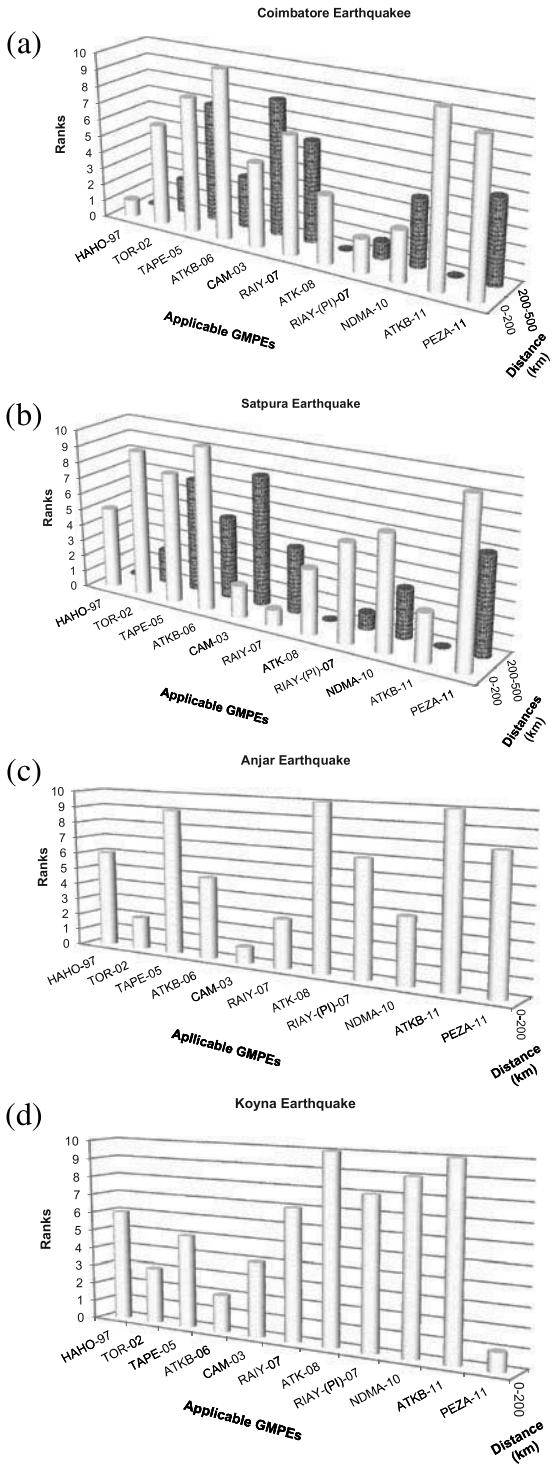

FIGURE 7 (a–k): 3-D Figure shows ranking GMPEs in each earthquakes in PI considering 0–200 km and 200–500 km segmented distance. Suitable GMPEs with weights for seismic hazard analysis in each earthquake region in given in Table 6.

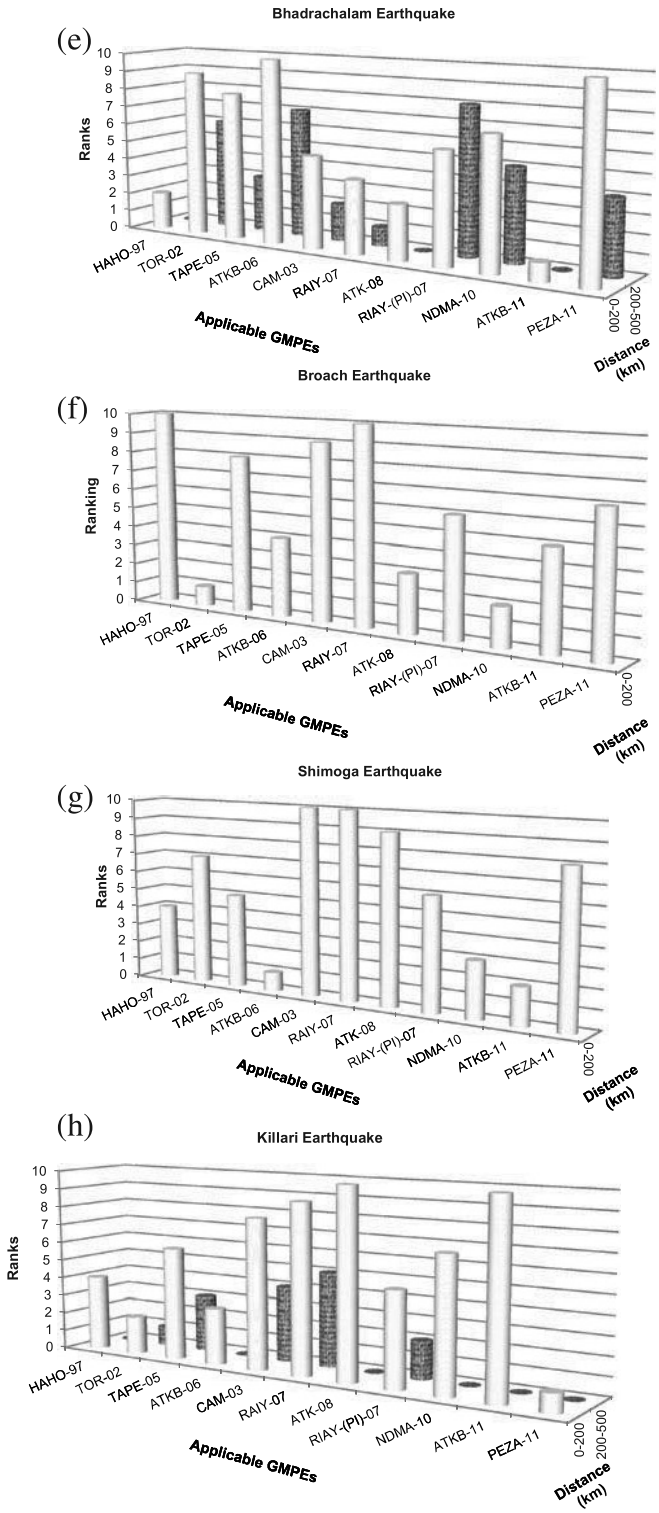

FIGURE 7 *(Continued).*

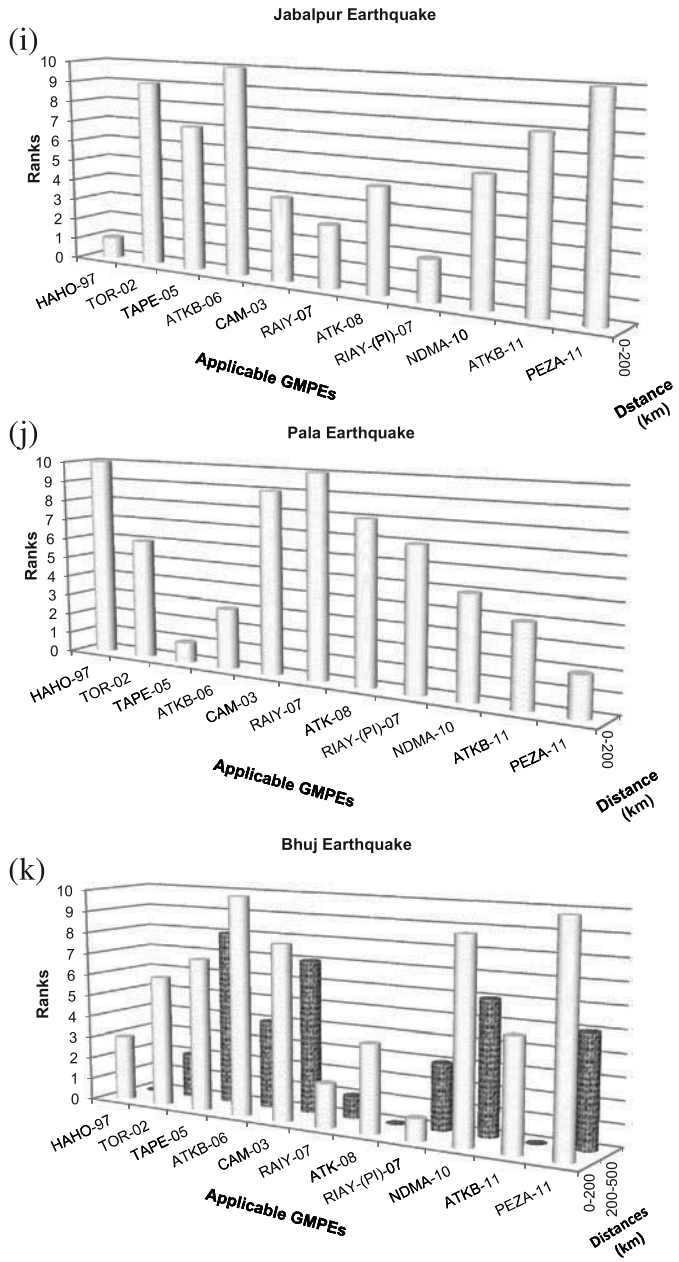

FIGURE 7 *(Continued).*

GMPE. It can be noted that ranking given in this study is slightly different from Nath and Thingbaijam [2011] for the same region. It can be noted from Table 2 that many widely used GMPEs with higher weights for SHA in PI (see Table 2) have not surfaced in our study. The segmented approach proposed in this study clearly determines the best suitable equations for 0–200 and 200-maximum damage distance as the rankings obtained from conventional method cannot be used for distances greater than 300 km. The best suitable GMPEs for each region of PI from this study in are given in Table 6. Figure 8 shows ranking order of GMPEs

TABLE 6 Suitable GMPEs for different parts of PI withData Support Index (DSI),Weights (W)and ranking order for different distance segment

		0–200 km			200-maximum damage distance km		
Earthquake name	GMPEs	DSI	W	Rank	DSI	W	Rank
	HAHO-97	53.5363	0.195	1		NA	
	TOR-02	3.4246	0.131	6	91.7751	0.319	2
	TAPE-05	−22.698	NC	NR	−76.521	NC	NR
	ATKB-06	−57.704	NC	NR	59.0428	0.265	3
	CAM-03	19.6301	0.152	5	−78.245	NC	NR
	RAIY-07	−0.0983	NC	NR	−57.972	NC	NR
	ATK-08	27.3306	0.162	4		*NA*	
Coimbatore 1900	RAIY-[PI]-07	53.5043	0.195	2	148.874	0.415	1
	NDMA-10	29.1081	0.164	3	−40.15	NC	NR
	ATKB-11	−68.822	NC	NR		*NA*	
	PEZA-11	−37.211	NC	NR	−46.803	NC	NR
	HAHO-97	9.521	0.118	5		NA	
	TOR-02	−53.227	NC	NR	0.096	0.153	2
	TAPE-05	−12.255	NC	NR	−98.107	NC	NR
	ATKB-06	−96.706	NC	NR	−64.536	NC	NR
	CAM-03	57.632	0.17	2	−98.822	NC	NR
Satpura 1938	RAIY-07	71.195	0.185	1	−58.823	NC	NR
	ATK-08	40.321	0.152	4		NA	
	RAIY-[PI]-07	3.971	0.112	6	455.674	0.847	1
	NDMA-10	1.076	0.109	7	−38.651	NC	NR
	ATKB-11	41.253	0.153	3		NA	
	PEZA-11	−62.781	NC	NR	−96.829	NC	NR
Anjar 1956	HAHO-97	−1.981	NC	NR			
	TOR-02	25.713	0.176	2			

(*Continued*)

TABLE 6 (Continued)

Earthquake name	GMPEs	0–200 km			200-maximum damage distance km		
		DSI	W	Rank	DSI	W	Rank
	TAPE-05	−62.261	NC	NR			
	ATKB-06	−1.572	NC	NR			
	CAM-03	275.583	0.527	1			
	RAIY-07	7.559	0.151	3	DATA NOT AVILABLE		
	ATK-08	−83.765	NC	NR			
	RAIY-[PI]-07	−10.365	NC	NR			
	NDMA-10	4.401	0.146	4			
	ATKB-11	−99.292	NC	NR			
	PEZA-11	−54.018	NC	NR			
Koyna 1967	HAHO-97	0.944	0.113	6			
	TOR-02	68.076	0.189	3			
	TAPE-05	13.742	0.128	5			
	ATKB-06	85.856	0.209	2			
	CAM-03	33.307	0.15	4			
	RAIY-07	−6.803	NC	NR	DATA NOT AVILABLE		
	ATK-08	−99.011	NC	NR			
	RAIY-[PI]-07	−22.393	NC	NR			
	NDMA-10	−61.521	NC	NR			
	ATKB-11	−100	NC	NR			
	PEZA-11	87.805	0.211	1			
Bhadrachalam 1969	HAHO-97	108.589	0.266	2	NA		
	TOR-02	−76.831	NC	NR	−64.281	NC	NR
	TAPE-05	−59.526	NC	NR	29.661	0.217	3
	ATKB-06	−98.311	NC	NR	−75.091	NC	NR

	CAM-03	−8.204	NC	NR	71.089	0.286	2
	RAIY-07	40.603	0.179	4	91.156	0.319	1
	ATK-08	72.43	0.22	3		NA	
	RAIY-[PI]-07	−25.443	NC	NR	−51.644	NC	NR
	NDMA-10	−28.004	NC	NR	−7.677	NC	NR
	ATKB-11	162.585	0.335	1		NA	
	PEZA-11	−87.499	NC	NR	6.788	0.178	4
Broach 1970	HAHO-97	−30.955	NC	NR			
	TOR-02	39.701	0.218	1			
	TAPE-05	−25.046	NC	NR			
	ATKB-06	22.734	0.192	4			
	CAM-03	−29.449	NC	NR			
	RAIY-07	−42.197	NC	NR	DATA NOT AVILABLE		
	ATK-08	26.996	0.198	3			
	RAIY-[PI]-07	−6.026	NC	NR			
	NDMA-10	38.027	0.215	2			
	ATKB-11	13.268	0.177	5			
	PEZA-11	−7.051	NC	NR			
Shimoga 1975	HAHO-97	−77.373	NC	NR			
	TOR-02	−90.995	NC	NR			
	TAPE-05	−87.289	NC	NR			
	ATKB-06	592.421	0.727	1			
	CAM-03	−99.985	NC	NR			
	RAIY-07	−99.979	NC	NR	DATA NOT AVILABLE		
	ATK-08	−98.267	NC	NR			
	RIAY-[PI]-07	−87.706	NC	NR			
	NDMA-10	−12.159	NC	NR			
	ATKB-11	159.535	0.273	2			
	PEZA-11	−98.197	NC	NR			

(*Continued*)

TABLE 6 (Continued)

		0–200 km			200-maximum damage distance km		
Earthquake name	GMPEs	DSI	W	Rank	DSI	W	Rank
Killari 1993	HAHO-97	18.547	0.13	4		NA	
	TOR-02	19.611	0.131	2	75.664	0.418	1
	TAPE-05	9.512	0.12	6	26.084	0.3	3
	ATKB-06	18.575	0.13	3	Insufficient Data		
	CAM-03	2.635	0.112	8	12.57	0.268	4
	RAIY-07	−12.265	NC	NR	−20.532	NC	NR
	ATK-08	−24.311	NC	NR		NA	
	RAIY-[PI]-07	16.991	0.128	5	72.718	0.411	2
	NDMA-10	7.421	0.118	7	Insufficient Data		
	ATKB-11	−77.358	NC	NR		NA	
	PEZA-11	20.643	0.132	1	Insufficient Data		
Jabalpur 1997	HAHO-97	51.391	0.189	1			
	TOR-02	−34.051	NC	NR			
	TAPE-05	−0.725	NC	NR			
	ATKB-06	−90.096	NC	NR			
	CAM-03	31.865	0.165	4			
	RAIY-07	39.065	0.174	3	DATA NOT AVILABLE		
	ATK-08	24.58	0.156	5			
	RAIY-[PI]-07	40.527	0.176	2			
	NDMA-10	13.118	0.141	6			
	ATKB-11	−23.099	NC	NR			
	PEZA-11	−52.573	NC	NR			
Pala 2000	HAHO-97	−37.396	NC	NR			
	TOR-02	3.813	0.13	6			

	TAPE-05	68.546	0.211	1				
	ATKB-06	39.181	0.174	3				
	CAM-03	−33.429	NC	NR	DATA NOT AVILABLE			
	RAIY-07	−73.727	NC	NR				
	ATK-08	−30.131	NC	NR				
	RAIY-[PI]-07	−24.153	NC	NR				
	NDMA-10	15.169	0.144	5				
	ATKB-11	17.608	0.147	4				
	PEZA-11	54.522	0.193	2				
Bhuj 2001	HAHO-97	16.158	0.164	3		NA		
	TOR-02	−19.786	NC	NR	156.855		0.351	2
	TAPE-05	−30.298	NC	NR	−99.325		NC	NR
	ATKB-06	−78.049	NC	NR	−51.928		NC	NR
	CAM-03	−34.578	NC	NR	−97.716		NC	NR
	RAIY-07	39.53	0.197	2	251.257		0.48	1
	ATK-08	6.215	0.15	4		NA		
	RAIY-[PI]-07	244.755	0.488	1	23.416		0.169	3
	NDMA-10	−44.113	NC	NR	−95.225		NC	NR
	ATKB-11	−16.065	NC	NR		*NA*		
	PEZA-11	−83.755	NC	NR	−87.333		NC	NR

Note: 1) NA: - Not Applicable; 2) NC: - Not considered; 3) NR: - Not Ranked.

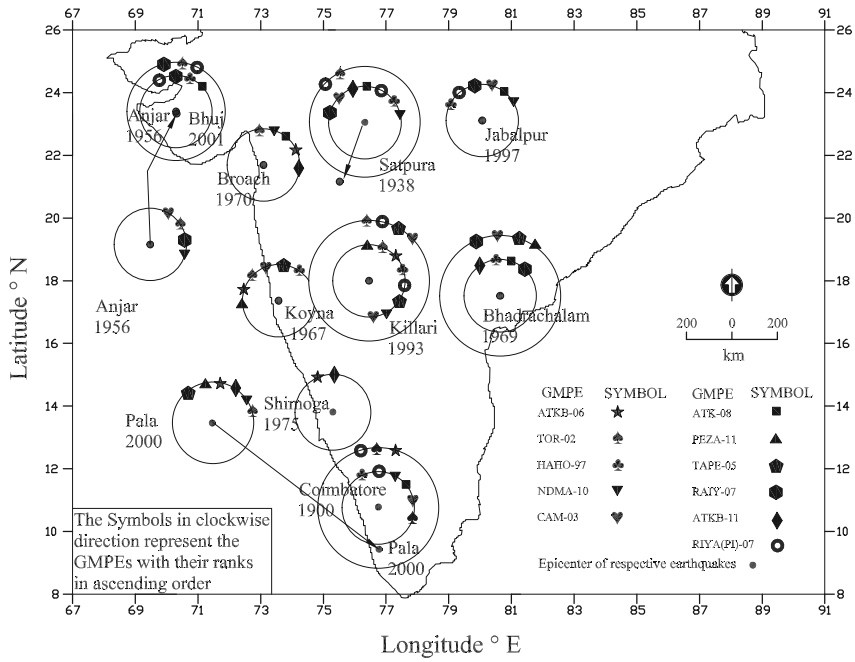

FIGURE 8 Ranking order (clockwise direction) of GMPEs for different region of PI.

(clockwise direction) for each segmented distance for different region in PI. The weights of each GMPEs plays an important role in the final hazard values. Theoretical methods proposed by Delavaud *et al.* [2009, 2012b] is not only useful in selecting the best ground motions models, but also helps to determine weights for each GMPE for SHA. A weight of each supporting GMPE has been estimated considering maximum past earthquake in the region. List of GMPEs suitable for each region/past earthquake with respective weights is given in Table 6. Conventional ranking system (0–300 km) gives almost uniform weights and segmented distance ranking shows considerable weight difference between GMPEs. This segmented distance ranking system will be more appropriate to select ground motion models for seismic hazard analysis for any region. Due to non-availability of recorded ground motion data, the present study used past EMS values to rank GMPEs. These results may be revisited in future if more rerecorded ground motion data are available.

8. Conclusions

This study presented suitable GMPEs for different part of PI considering the past earthquakes. About 11 GMPEs are available for any part of PI. Efficacy analysis was carried out by considering magnitude, depth, and hypocentral distance of each earthquake. Log-likelihood value was estimated for each GMPE for given earthquake data, which are used to estimate data support index and weights of all applicable GMPEs. Data support index values are used to select supporting GMPEs for maximum past earthquakes in the region. GMPEs with positive DSI are considered as the best suitable GMPEs for seismic hazard analysis in the region. Ranks and weights of supporting GMPE for different parts of PI are presented. In this paper GMPE ranking has been carried out considering segmented distance based on maximum damaged distance from Isoseismal map. Entire maximum

damaged distance was divided into two segments 0–200 km and 200-maximum damage distance. This study showed that the 0–300 km ranking system rejects or promotes ranks of GMPEs valid up to 200 km, but segmented ranking accounts all GMPEs applicable for region in appropriate position. Segmented distance ranking proposed in this paper accounts all GMPEs and supports appropriate GMPEs for each segments based on information-theoretic approach. Comparison between 0–300 km ranking and segmented distance ranking shows considerable difference in ranks. Segmented distance ranking can be adopted for long as well as short distance hazard estimation. Ranks and weights of the best suitable GMPEs for different part of PI are presented.

Acknowledgment

The authors personally thank Dr. E. Delavaud and Dr. K.K. S. Thingbaijam for their valuable suggestions during GMPE analysis.

Funding

The authors would like to extend their sincere appreciation to the Deanship of Scientific Research at King Saud University for funding Research group NO.(RG -1435-09).

References

Abrahamson, N. A. and Silva, W. J. [1997] "Empirical response spectral attenuation relations for shallow crustal earthquakes," *Seismological Research Letters* **68**(1), 94–127.

Algermissen, S. T. and Perkins, D. M. [1976] "A probabilistic estimate of maximum acceleration in rock in the contiguous United States," U.S. Geology Survey Open-file Report **45**, 76–416.

Anbazhagan, P. [2007] "Site characterization and seismic hazard analysis with local site effects for microzonation of Bangalore," Ph.D. dissertation, Indian Institute of Science, Bangalore, India.

Anbazhagan, P., Vinod, J. S., and Sitharam, T. G. [2009] "Probabilistic seismic hazard analysis for Bangalore," *Journal of Natural Hazards* **48**, 145–166.

Anbazhagan, P., Prabhu, G., and Aditya, P. [2012] "Seismic Hazard Map of Coimbatore using Subsurface Fault Rupture," *Natural Hazards* **60**, 1325–1345.

Atkinson, G. M. and Boore, D. M. [1995] "Ground-motion relations for Eastern North America," *Bulletin of the Seismological Society of America* **85**(1), 17–30.

Atkinson, G. M. and Boore, D. M. [1997] "Some comparisons between recent ground motion relations," *Seismological Research Letters* **68**(1), 24–40.

Atkinson, G. M. and Boore, D. M. [2006] "Earthquake ground-motion predictions for Eastern North America," *Bulletin of the Seismological Society of America* **96**, 2181–2205.

Atkinson, G. M. [2008] "Ground-motion prediction equations for Eastern North America from a referenced empirical approach: implications of epistemic uncertainty," *Bulletin of the Seismological Society of America* **98**, 1304–1318.

Atkinson, G. M. and Boore, D. M. [2011] "Modifications to existing ground-motion prediction equations in light of new data," *Bulletin of the Seismological Society of America* **101**(3), 1121–1135.

Basu, S., and Nigam, N. C. [1977] "Seismic risk analysis of Indian peninsula," *Proc. of Sixth World Conference on Earthquake Engineering*, New Delhi, **1**, 782–788.

Boore, D. M., Joyner, W. B., and Fumal, T. E. [1997] "Equations for estimating horizontal response spectra and peak acceleration from Western North American earthquakes: a summary of work," *Seismological Research Letters* **68**(1), 128–153.

Bhatia, S. C., Kumar, M. R., and Gupta, H. K. [1999] "A probabilistic seismic hazard map of India and adjoining regions," *Annali di Geofisica* **42**(1), 153–1,166.

Biswal, T. K., De Waele, B., and Ahuja, H. [2007] "Timing and dynamics of the juxtaposition of the Eastern Ghats Mobile belt against the Bhandara Craton, India: a structural and zircon U–Pb SHRIMP study of the fold-thrust belt and associated nephelinesyenite plutons," *Tectonics* **26**, 1–21.

Bodin, P., Malagnini, L., and Akinci, A. [2004] "Ground motion scaling in the Kachchh Basin, India, deduced from aftershocks of the 2001 M_w 7.6 Bhuj earthquake," *Bulletin of the Seismological Society of America* **94**, 1658–1669.

Bommer, J. J., Scherbaum, F., Bungum, H., Cotton, F., Sabetta, F., and Abrahamson, N. A. [2005] "On the use of logic trees for ground-motion prediction equations in seismic-hazard analysis," *Bulletin of the Seismological Society of America* **95**, 377–389.

Bommer, J. J., Douglas, J., Scherbaum, F., Cotton, F., Bungum, H., and Fäh, D. [2010] "On the selection of ground motion prediction equation for seismic hazard analysis," *Seismological Research Letters* **81**, 5.

Boore, D. M., Atkinson, G. M., and Eeri, M. [2008] "Ground-motion prediction equations for the average horizontal component of PGA, PGV and 5% damped PSA at spectral periods between 0.01 s and 10.0 s," *Earthquake Spectra* **24**(1), 99–138.

Braun, I., Cenki-Tok, B., Paquette, J. L., and Tiepolo, L. [2007] "Petrology and U–Th–Pb geochronology of the sapphirine–quartz-bearing metapelites from Rajapalayam, Madurai Block, southern India: evidence for polyphase Neoproterozoichigh grade metamorphism," *Chemical Geology* **241**, 129–147.

Campbell, W. K. [1997] "Empirical near-source attenuation relationships for horizontal and vertical components of peak ground acceleration, peak ground velocity and pseudo-absolute acceleration response spectra," *Seismological Research Letters* **68**(1), 154–179.

Campbell, K. W. [2003] "Prediction of strong ground motion using the hybrid empirical method and its use in the development of ground-motion (attenuation) relations in Eastern North America," *Bulletin of the Seismological Society of America* **93**, 1012–1033.

Campbell, K. W. and Bozorgnia, Y. [2008] "NGA ground motion model for the geometric mean horizontal component of PGA, PGV, PGD and 5% damped linear elastic response spectra for period ranging from 0.01to 10s," *Earthquake Spectra* **24**, 139–171.

Chandra, U. [1977] "Earthquakes of peninsula India: a seismotectonic study," *Bulletin of the Seismological Society of America* **67**, 1387–1413.

Chaudhuri, A. K. [2003] "Stratigraphy and paleogeography of the Godavari Supergroup in the south-central Pranhita-Godavari Valley, south India," *Journal of Asian Earth Sciences* **21**, 595–611.

Chetty, T. R. K. and Rao, Y. J. B. [2006] "The Cauvery shear zone, southern granulite terrane, India: a crustal scale flower structure," *Gondwana Research* **10**, 77–85.

Corigliano, M., Lai, C. G., Menon, A., and Ornthammarath, T. [2012] "Seismic input at the archaeological site of Kancheepuram in Southern India," *Natural Hazard* **63**(2), 845–866.

Cotton, F., Scherbaum, F., Bommer, J. J., and Bungum, H. [2006] "Criteria for selecting and adjusting ground-motion models for specific target regions: application to Central Europe and rock sites," *Journal of Seismology* **10**, 137–156.

Cramer, C. H. and Kumar, A. [2003] "2001 Bhuj, India, earthquake engineering seismoscope recordings and eastern North America ground motion attenuation relations," *Bulletin of the Seismological Society of America* **93**, 1390–1394.

Delavaud, E., Scherbaum, F., Kuehn, N., and Riggelsen, C. [2009] "Information-theoretic selection of Ground-motion Prediction equations for Seismic hazard analysis: an applicability study using Californian data," *Bulletin of the Seismological Society of America* **99**, 3248–3263

Delavaud, E., Scherbaum, F., Kuehn, N., and Allen, T. [2012a] "Testing the global applicability of ground-motion prediction equations for active shallow crustal regions," *Bulletin of the Seismological Society of America* **102**(2) 702–721.

Delavaud, E., Cotton, F., Akkar, S., Scherbaum, F., Danciu, L., Beauval, C., Drouet, S., Douglas, J., Basili, R., Abdullah, M.S., Segou, M., Faccioli, E., and Theodoulidis, N. [2012b] "Toward a ground-motion logic tree for probabilistic seismic hazard assessment in Europe," *Journal of Seismology* **16**(3), 451–473.

Douglas, J. [2010] "Consistency of ground-motion predictions from the past four decades," *Bulletin of Earthquake Engineering* **8**, 1515–1526.

Frankel, A., Mueller, C., Barnhard, T., Perkins, D., Leyendecker, E., Dickman, N., Hanson, S., and Hopper, M. [1996] "National seismic hazard maps: Documentation June 1996, U.S.," Geological Survey Open-file Report 96-532, 110 pp. (Available at http://eqhazmaps.usgs.g0v).

Ghosh, B., Pappin, J. W., So M. M. L., and Hicyilmaz K. M. O. [2012] "Seismic hazard assessment in India," *Proc. of the Fifteenth World Conference on Earthquake Engineering*, Lisbon, Portugal.

Grünthal, G. [1998] "European macroseismic scale 1998," Cahiers du Centre Européen de Géodynamiqueet de Séismologie 15, Luxembourg.

Guha, S. K. and Basu, P. C. [1993] "Catalogue of earthquakes M C 3.0 in peninsular India," Atomic Energy Regulatory Board. Tech. Document No. TD/CSE-1, 1–70.

Gupta, H. K. [2006] "Stable continental regions are more vulnerable to earthquake than once thought," *Journal of Indian Geophysics Union* **10**, 59–61; Eos, *Transactions, America Geophysical Union* **79**(27), 319–321.

Hintersberger, E., Scherbaum, F., and Hainzl, S. [2007] "Update of likelihood-based ground-motion model selection for seismic hazard analysis in western central Europe," *Bulletin of Earthquake Engineering* **5**, 1–16.

Hwang, H. and Huo, J. R. [1997] "Attenuation relations of ground motion for rock and soil sites in eastern United States," *Soil Dynamics and Earthquake Engineering* **16**, 363–372.

Iyengar R. N. and Raghukanth S. T. G. [2004] "Attenuation of strong ground motion in peninsular India," *Seismological Research Letters* **75**(4), 530–540.

Jaiswal, K. and Sinha R. [2007a] "Probabilistic seismic hazard estimation for peninsular India," *Bulletin of the Seismological Society of America* **97**(1), 318–330.

Jaiswal, K. and Sinha, R. [2007b] "Spatial variation of maximum considered and design basis earthquakes in peninsular India," *Current Science* **92**(5), 639–645.

Jaiswal, K. and Sinha, R. [2008] "Spatial-temporal variability of seismic hazard in peninsular India," *Journal of Earth System Science* **117**(S2), 707–718.

Joyner, W. B. and Boore, D. M. [1981] "Peak horizontal acceleration and velocity from strong-motion records including records from the 1979 Imperial Valley, California, Earthquake," *Bulletin of the Seismological Society of America* **71**, 2011–2038.

Kanagarathinam, L., Dodagoudar, G. R., and Boominathan A. [2008] "Probabilistic seismic hazard studies of east coast region of India," *The 14th World Conference on Earthquake Engineering*, October 12–17, Beijing, China.

Khattri, K. N., Rogers A. M., Perkins D. M., and Algermissen, S. T. [1984] "A seismic hazard map of India and adjacent areas," *Tectonophysics* **108**, 93–134.

Kolathayar, S. and Sitharam, T. G. [2012] "Characterization of regional seismic source zones in and around India," *Seismological Research Letters* **83**(1), 78–85.

Kramer, S. L. [1996] *Geotechnical Earthquake Engineering*, Pearson Education Ltd., Reprinted 2003, Delhi, India.

Lalith Kumar, B. V. K., Rao, G. V. R., and Rao, K. S. [2012] "Seismic hazard analysis of low seismic regions, Vishakhapatnam: probabilistic approach," *Journal of Indian Geophysics Union* **16**(1), 11–20.

Martin, S. and Szeliga, W. [2010] "A catalog of felt intensity data for 589 earthquakes in India1636–2008," *Bulletin of the Seismological Society of America* **100**(2), 562–569.

Meert, J. G., Pandit, M. K., Pradhan, V. R., Banks, J., Sirianni, R., Stroud, M., Newstead, B., and Gifford, J. [2010] "Precambrian crustal evolution of Peninsular India: A 3.0 billion year odyssey," *Journal of Asian Earth Sciences* **39**, 483–515.

Menon, A., Ornthammarath, T., Corigliano, M., and Lai, C. G. [2010] "probabilistic seismic hazard macrozonation of Tamil Nradu in Southern India," *Bulletin of the Seismological Society of America* **100**(3), 1320–1341.

Nath, S. K. and Thingbaijam, K. K. S. [2011] "Peak ground motion predictions in India: an appraisal for rock sites," *Journal of Seismology* **15**(2), 295–315.

Nath, S. K. and Thingbaijam, K. K. S. [2012] "Probabilistic seismic hazard assessment of India," *Seismological Research Letters* **83**(1), 135–149.

NDMA (National Disaster Management Authority) [2010] "Development of probabilistic seismic hazard map of India," Technical Report Publicised by Govt. of India, New Delhi, Working committee of experts (WCE), NDMA.

Petersen, M. D., Rastogi, B. K., Schweig, E. S., Harmsen, S. C., and Gomberg, J. S. [2004] "Sensitivity analysis of seismic hazard for the north-western portion of the state of Gujarat, India," *Tectonophysics* **390**, 105–115.

Pezeshk, S., Zandieh, A., and Tavakoli, B. [2011] "Hybrid empirical ground-motion prediction equations for Eastern North America using NGA models and updated seismological parameters," *Bulletin of the Seismological Society of America* **101**(4), 1859–1870.

Raghukanth, S. T. G. and Iyengar, R. N. [2007] "Estimation of seismic spectral acceleration in peninsular India," *Journal of Earth System Science* **116**(3), 199–214.

Raith, M. M., Srikantappa, C., Buhl, D., and Koehler, H. [1999] "The Nilgirienderbites, South India; nature and age constraints on protolith formation, high-grade metamorphism and cooling history," *Precambrian Research* **98**, 129–150.

Ramanna, C. K. and Dodagoudar, G. R. [2012] "Seismic hazard analysis using the adaptive kernel density estimation technique for Chennai City," *Pure and Applied Geophysics* **169**, 55–69.

Rao, B. R. and Rao, P. S. [1984] "Historical seismicity of peninsular India," *Bulletin of the Seismological Society of America* **74**(6), 2519–2533.

Rollinson, H. R., Windley, B. F., and Ramakrishnan, M. [1981] "Contrasting high and intermediate pressures of metamorphism in the Archaean Sargur Schists of southern India," *Contributions to Mineralogy and Petrology* **76**, 420–429.

Roshan, A. D. and Basu, P. C. [2010] "Application of PSHA in low seismic region: a case study on NPP site in peninsular India," *Nuclear Engineering Design* **240**, 3443–3454.

Sabetta, F., Lucantoni, A., Bungum, H., and Bommer, J. J. [2005] "Sensitivity of PSHA results to ground motion prediction relations and logic-tree weights," *Soil Dynamics and Earthquake Engineering* **25**, 317–329.

Sadigh, K., Chang, C. Y., Egan, J. A., Makdisi, F., and Youngs, R.R. [1997] "Attenuation relations for shallow crustal earthquakes based on California strong motion data," *Seismological Research Letters* **68**(1), 180–189.

Santosh, M., Collins, A. S., Tamashiro, I., Koshimoto, S., Tsutsumi, Y., and Yokoyama, K. [2006] "The timing of ultrahigh-temperature metamorphism in southern India: U–Th–Pb electron microprobe ages from zircon and monazite in sapphirine bearing granulites," *Gondwana Research* **10**, 128–155.

Scherbaum, F., Cotton, F., and Smit, P. [2004] "On the use of response spectral reference data for the selection and ranking of ground-motion models for seismic hazard analysis in regions of moderate seismicity: the case of rock motion," *Bulletin of the Seismological Society of America* **94**, 1–22.

Scherbaum, F., Bommer, J. J., Bungum, H., Cotton. F., and Abrahamson, N. A. [2005] "Composite ground-motion models and logic trees: methodology, sensitivities, and uncertainties," *Bulletin of the Seismological Society of America* **95**, 1575–1593.

Scherbaum, F., Delevaud, E., and Riggelsen, C. [2009] "Model selection in Seismic hazard analysis: an information theoretic earthquake source models," *Bulletin of the Seismological Society of America* **94**, 1053–1069.

Schweig, E., Gomberg, J., Petersen, M., Ellis, M., Bodin, P., Mayrose, L., and Rastogi, B. K. [2003] "The Mw 7.7 Bhuj Earthquake: Global lessons for earthquake hazard in intra-plate regions," *Journal of the Geological Society of India* **61**(3), 277–282.

Shukla J. and Choudhury D. [2012] "Estimation of seismic ground motions using deterministic approach for major cities of Gujarat", Na*tural Hazards and Earth System Sciences* **12**, 2019–2037.

Sitharam, T. G., Vipin, K. S., and Ganesha R. K. [2012] "A study on Seismicity and Seismic Hazards for the Karnataka State," *Journal of Earth System Sciences* **121**(2), 475–490.

Sitharam, T. G. and Kolathayar, S. [2013] "Seismic hazard analysis of India using areal sources," *Journal of Earth Sciences* **62**, 647–653.

Srivastava, H. N. and Ramachandran, K. [1985] "New catalog of earthquakes for peninsular India during 1839–1900" *Mausam* **36**(3), 351–358.

Stein, H. J., Hannah, J. L., Zimmerman, A., Markey, R. J., Sarkar, S. C., and Pal, A. B. [2004] "A 2.5 Ga porphyry Cu–Mo–Au deposit at Malanjkhand, central India; implications for late Archean continental assembly," *Precambrian Research* **134**, 189–226.

Strasser, F. O., Abrahamson, N. A., and Bommer, J. J. [2009] "Sigma: Issues, insights, and challenges," *Seismological Research Letters* **80**(1), 40–56.

Szeliga, W., Hough, S. E., Martin, S., and Bilham, R. [2010] "Intensity, magnitude, location, and attenuation in India for felt earthquakes since 1762," *Bulletin of the Seismological Society of America* **100**(2), 570–584.

Tavakoli, B. and Pezeshk, S. [2005] "Empirical-stochastic ground motion prediction for Eastern North America," *Bulletin of the Seismological Society of America* **95**, 2283–2296.

Tewari, H. C., Murty, A. S. N., Prakash, K., and Sridhar, A. R. [2001] "A tectonic model of the Narmada region," *Current Science* **80**(7), 873–878.

Thaker, T. P., Rao, K. S., and Gupta, K. K. [2010] "Seismic hazard analysis for Surat City and its surrounding region, Gujarat," *Indian Geotechnical Conference*, Bombay, pp. 163–166.

Toro, G. R., Abrahamson, N.A., and Schneider, J.F. [1997] "A model of strong ground motions from earthquakes in Central and Eastern North America: Best estimates and uncertainties," *Seismological Research Letters* **68**(1), 41–57.

Toro, G.R. [2002] "Modification of the Toro *et al*. (1997) attenuation equations for large magnitudes and short distances," *Technical Report*, Risk Engineering.

Vipin, K. S., Anbazhagan, P., and Sitharam, T. G. [2009] "Estimation of peak ground acceleration and spectral acceleration for south India with local site effects: Probabilistic approach," *Natural Hazards Earth System Science* **9**, 865–878.